A Study of the Pressure-Penetration Relationship For Model Footings on Cohesive Soil

W. H. PERLOFF and K. S. A. RAHIM
Respectively, Associate Professor of Soil Mechanics, Purdue University; and Research Associate, Department of Civil Engineering, Ohio State University

This paper describes a study of the relationship between the pressure on model footings and the penetration of these footings into saturated cohesive soils. Experimental results demonstrate the influence of soil water content, rate of footing penetration, type of testing, and roughness of the footing base on this relationship. An empirical expression has been developed to describe the pressure-penetration relationship. At this time, the empirical equation represents the data satisfactorily for square, rectangular, circular, and elliptical model footings of various sizes.

•THE RESULTS of small-scale footing penetration tests are frequently utilized to predict the sinkage of off-road vehicles traveling on soft soils. Inasmuch as the resistance which the soil offers to motion is intimately related to the vehicle sinkage, an adequate description of cross-country mobility depends on the ability to predict sinkage of the prototype vehicle. However, to do this, it must be possible to express the pressure-penetration relationship for a loaded area on the soil in terms of appropriate scale factors.

The problem is somewhat different from that often considered by foundation engineers, because the magnitude of sinkage experienced by vehicles on soft soils is greatly in excess of that which can be tolerated by most civil engineering structures. One relationship commonly used in the field of land locomotion mechanics is that suggested by Bekker (2):

$$p = \left(\frac{k_c}{b} + k_\phi\right) z^n \tag{1}$$

where k_c is the cohesive modulus of deformation of the soil, k_ϕ is the frictional modulus of deformation of the soil, b is the width of the loaded area, z is the sinkage of the area, n is a dimensionless exponent, and p is the pressure applied to the area. Many efforts have been made to verify this equation and to correlate the parameters k_c and k_ϕ to soil type (9, 28, 29).

However, Eq. 1 can be questioned on several counts. Theoretical analyses of rigid (3) and flexible (23, 30, 31) loaded areas on semi-infinite elastic media, as well as experimental results for rigid loaded areas on both sands and clay (4, 7, 10, 11) indicate that the displacement of a loaded plate on a soil is a function not only of the width of the plate but of the shape as well. In addition, the interpretation of k_c and k_ϕ as meaningful soil behavior parameters is hampered by the fact that the dimensions of these constants are a function of the exponent n, which is a function of plate size and soil type. Hence, even for a given soil, the deformation moduli will have different dimensions. Furthermore, it would seem appropriate to examine critically the form

Paper sponsored by Committee on Foundations of Bridges and Other Structures and presented at the 45th Annual Meeting.

of the equation. Osterberg (17) found a straight-line load-sinkage relationship on a logarithmic plot, for load tests on clay, only in the range of small penetrations. Kondner and Krizek (11) suggest a hyperbolic relationship as most appropriate to fit their own data as well as those of other investigators. However, there is some question that the magnitude of deformation in the tests which they examined was sufficiently large to apply to a mobility problem. Vincent et al (29) suggested that Eq. 1 was valid for model plate studies on sand within a range of sinkage from 0.5 to 4.5 in. They found the exponent n to have a magnitude of approximately unity in this range, thus suggesting that the pressure-penetration relationship is linear! If such were the case over a meaningful range of pressures, the equations relating the pressure on a loaded area to the penetration of that area into the soil could be derived from finite elasticity theory. Clearly, the pressure-penetration relationship for soils is hardly this simple.

Based on the foregoing discussion, it seems that there is no presently available description of the pressure-penetration relationship for model footings on soil which is sufficiently general to encompass all of the significant factors involved. It was the specific objective of this study to examine this relationship for saturated cohesive soils, to elucidate the factors which influence it, and to seek an empirical description of the relationship.

PRELIMINARY ANALYSIS

In studying a problem in which so many factors affect the results, it is often convenient to group the factors into non-dimensional ratios. The standard method by which this is accomplished, dimensional analysis, has, in general, two benefits: first, it permits reduction in the number of variables studied; and second, it can assist the investigator in establishing dimensionless parameters of more significance to the problem than the individual factors themselves.

The variables thought to influence the pressure-penetration relationship for a purely cohesive soil ($\phi = 0$) are given in Table 1. Not all of the factors listed are independent. For example, the geometry of a footing can be described by the area, A, the circumference, C, and combinations of C, the width, B, and the length, L. Hence, when the independent variables have been chosen, they can be expressed in a variety of ways as non-dimensional ratios. Application of dimensional analysis procedures (12) yields functional relationships of the following general type:

$$f\left(\frac{z}{\sqrt{A}}, \frac{P}{Aq}, \frac{B}{L}, \frac{Pt}{A\eta}\right) = 0 \qquad (2)$$

TABLE 1

VARIABLES AFFECTING PRESSURE-PENETRATION RELATIONSHIP FOR SATURATED COHESIVE SOIL

Variable	Symbol	Dimensions
Footing width (or minor axis)	B	L
Footing length (or major axis)	L	L
Footing circumference	C	L
Footing area	A	L^2
Footing penetration	z	L
Force on footing	P	F
Soil water content	w	$F^0 L^0 T^0$
Soil strength parameter	q	FL^{-2}
Friction or adhesion coefficient between footing and soil	δ	$F^0 L^0 T^0$
Viscosity of soil	η	$FL^{-2}T$
Time of loading	t	T

One of the difficulties in a dimensional analysis approach is the choice of the most physically meaningful arrangement of variables. For example, the footing penetration can be represented in dimensionless form by any one of the following quantities:

$$\frac{z}{\sqrt{A}}, \frac{z}{B}, \frac{z}{C}, \frac{z}{L}, \frac{z}{\sqrt{CL}}, \frac{z}{\sqrt{CB}}$$

Similarly, the footing pressure can be expressed in a variety of ways, among which are

$$\frac{\sigma}{q}, \frac{\sigma t}{\eta}$$

where σ is the unit pressure on the footing (P/A).

The most useful parameters are determined from experimental results, and are discussed later.

EXPERIMENTAL PROCEDURES

Soil Used

The cohesive soil used in the majority of the tests was received as a dry, powdered, water-washed kaolin mined by the Edgar Plastic Kaolin Company of Edgar, Fla., and referred to herein as EPK. The clay is white, odorless when mixed with distilled water, and possesses the following classification properties:

Liquid limit: 58. 5 percent
Plastic limit: 36. 5 percent
Plasticity index: 22. 0 percent
Shrinkage limit: 27. 4 percent
Specific gravity of solids: 2. 597
Percent clay size (< 0. 002 mm): 78 percent

Preparation of Soil Material for Testing

The powdered EPK was mixed in the as-received condition with a sufficient quantity of distilled water to bring the water content to approximately 45 to 48 percent. Initial mixing to insure homogeneity was performed with a Blakeslee power mixer. The soil was then passed through a Vac-Aire sample extruder which forces the soil through small openings into an evacuated chamber, thus removing air trapped in the voids. This feature is very important, because the use of unsaturated soil would further complicate the problem. The soil was passed through the extruder a minimum of three times to insure complete saturation and promote homogeneity, and was then extruded through a 2-in. square die. A complete description of the extruder and its operation is presented by Matlock et al (13).

Samples were cut precisely to desired lengths to fit tightly into four testing bins ranging in size from 10 in. wide by 18 in. long by 10 in. deep to 30 in. wide by 36 in. long by 36 in. deep. The extruded soil prisms were placed side by side in the bin to form a single 2-in. thick layer. The box dimensions are arranged so that the soil prisms will fit tightly together to form a uniform mass. When each layer was completed it was tamped with a spring loaded 2-in. square tamper, to insure that the soil truly formed a continuous mass. The spring tamper exerts a pressure approximating 2 psi on the soil. By this method, a mass of reasonably homogeneous, fully saturated cohesive soil can be prepared. The degree of saturation of the soil was checked on several occasions, and the soil was saturated in all cases.

The required number of layers of soil were placed in the bin, tamped, and covered with several sheets of waterproof plastic. The bin of soil was stored for at least 12 hr in a humid room before testing, to permit any minor internal adjustments of water content, and to promote further uniformity.

Model Footings

The plan dimensions of the model footings tested range in size from 1 by 1 in. to 3 by 9 in. They include squares, rectangles, circles, and ellipses. Some of the 1- and 2-in. square footings were made of brass. All other footings were made of polished, case-hardened, cold-rolled steel. The sides of all footings were polished to a smooth finish. The bases of the smooth footings were also polished to a smooth surface, whereas the bases of the rough footings were grooved in two directions at right angles to each other.

The footings were rigidly attached to the loading device in such a way as to prevent any rotation during testing.

Testing Procedure

The footings were loaded by an Instron Model TT-BM-L, Universal Testing Machine. Footing loads and penetrations were continuously recorded by the Instron on a 10-in.

Figure 1. Penetration test in progress.

wide strip chart. Figure 1 shows the Instron Testing Machine with a model footing mounted on the load cell under the crosshead at the inception of a test.

Before the start of each test, the soil underneath the model footing was leveled, and the model footing was lubricated on all sides and the base with Dow-Corning 200 silicone fluid with a viscosity of 1,000 centipoise, except in the case of the rough base footings, where only the sides were lubricated. During the course of the test the surface of the soil was covered with a plastic sheet at all times, except in the immediate vicinity of the footing, to inhibit loss of moisture through evaporation.

When more than one footing was tested in a bin, the spacing between the footings was never less than three times the footing width.

During the course of this research, a total of 247 model footing tests were performed (20). The majority of the tests were performed at constant rates of penetration of 0.50 or 2.0 cm/min. However, some tests were run as slowly as 0.01 cm/min and others were performed as rapidly as 8 cm/min. In the case of the constant rate of loading tests, the loading rate was either 12.5 or 25 kg/min. As it was necessary to vary the rate of penetration continuously to maintain a constant rate of loading, the rate of loading was chosen so that the penetration rates encountered would cover approximately the range of rates studied in the constant penetration rate tests. The constant rate of loading tests were carried out with a special load pacing attachment for the Instron which permitted a continuous loading rather than requiring application of discrete load increments.

Figure 2 shows a 1- by 16-in. model footing which has penetrated the soil to a depth of approximately 5 in. For illustrative purposes, the load cell and mounting plate have

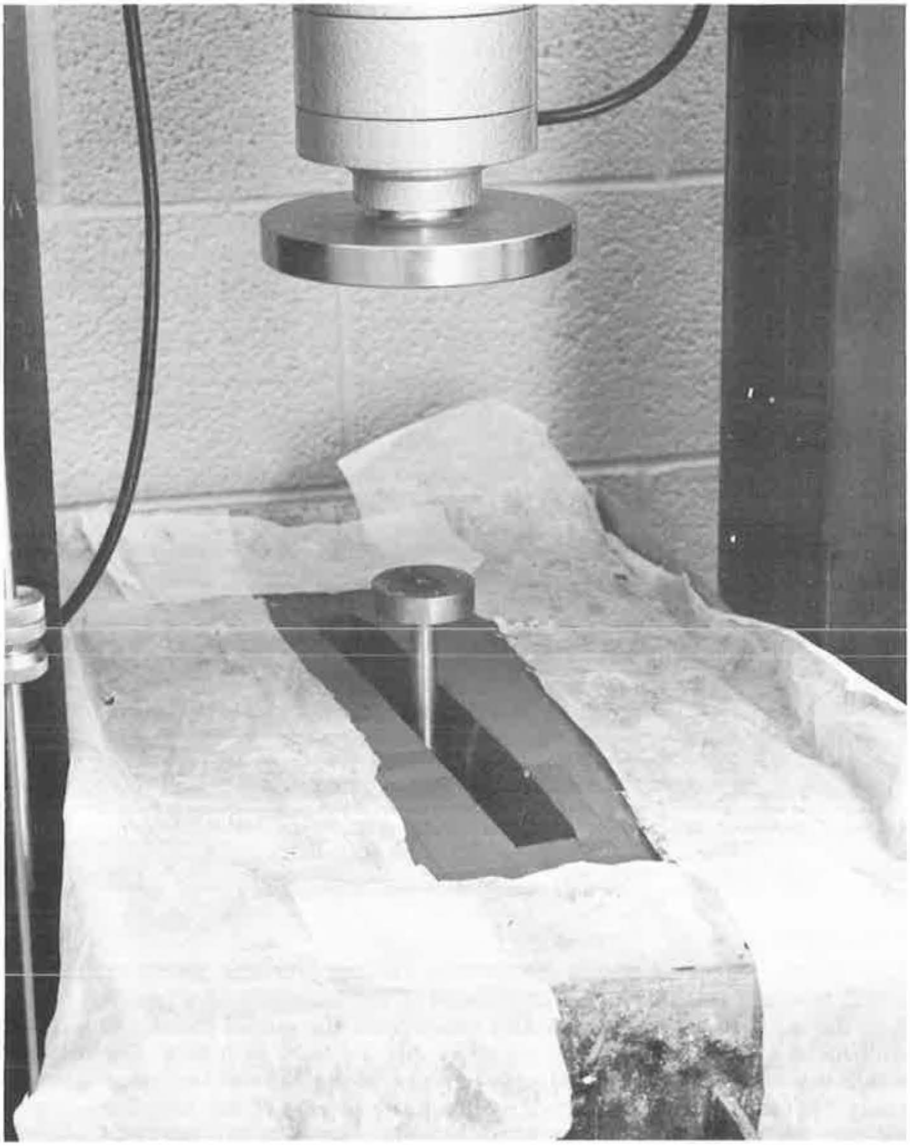

Figure 2. Model 1- by 16-in. footing at completion of penetration test.

been removed, and the footing has been left embedded in the soil. Bulging of the ground surface has occurred in the vicinity of the footing.

At the completion of each model footing test, small soil specimens were removed from the area immediately under the center and sides of the footing indentation, and the water content of these specimens was determined. At the completion of each series of footing tests, a 2-in. diameter cylindrical specimen was removed from the soil bin and an unconfined compression test performed on this specimen. Both ends of the unconfined test specimen were lubricated with silicone grease to minimize the influence of end restraint.

When each series of tests was completed, the remaining soil from the test bin was removed and thoroughly remixed with a sufficient quantity of freshly mixed soil to fill the test bin. The soil was then extruded once more, and a new test series prepared.

During the process of remixing, extrusion, and preparation of sample, approximately 1 to 2 percent of water was lost by evaporation. Thus, it was most convenient to prepare an initial batch of soil at a high water content and have subsequent batches at successively lower water contents.

FACTORS INFLUENCING EXPERIMENTAL RESULTS

In addition to the primary factors of footing shape and size, the following variables were felt to have a potentially significant influence on the pressure-penetration relationship: (a) water content of the soil, (b) rate of footing penetration, (c) type of testing, i.e., controlled rate of penetration or controlled rate of loading, and (d) roughness of the footing base.

Effect of Water Content

For most of the presently available results of model footings tests on cohesive soil, virtually no mention is made of the influence of water content. This seems to be the case because large batches of cohesive soil are usually tested in the unsaturated condition, and the problem is avoided by performing all tests under approximately identical conditions. In the writers' opinion, neglect of water content effects can lead to experimental errors which may obscure other effects being examined.

Figure 3 shows pressure-penetration curves for 2-in. square model footings on EPK at a variety of water contents. To some extent the shape, and certainly the ordinates of these curves, depend in an important way on the water content. These results are not surprising because the strength of EPK tested is greatly influenced by the water content. Since a model footing test is really only one form of strength test of the soil, it is to be expected that the pressure-penetration curves would be highly dependent on

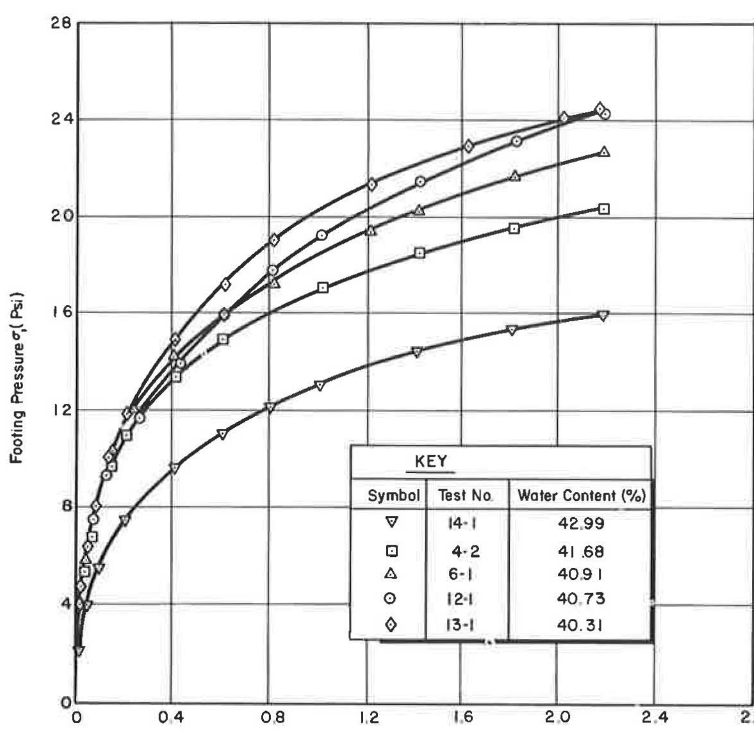

Figure 3. Effect of water content on pressure-penetration relationship for 2-in. square footings on EPK.

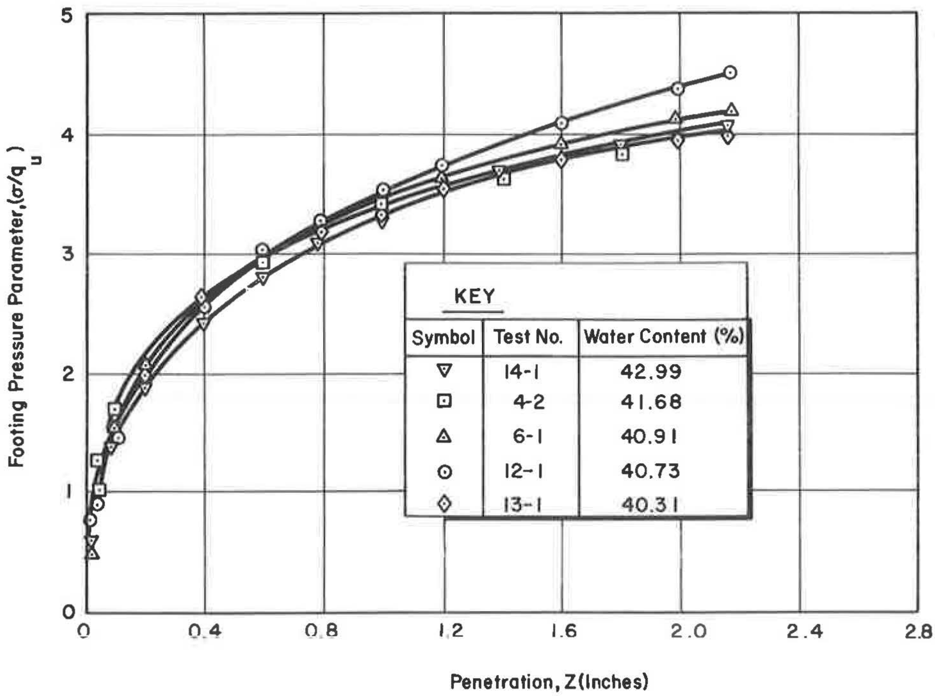

Figure 4. Effect of water content on pressure parameter-penetration relationship for 2-in. square footings on EPK.

water content effects. One way to assist in reducing the influence of water content on test results is suggested by the dimensional analysis previously described and by Kondner and Krizek (11). Inasmuch as the strength might be expected to depend on water content in the same general way as the pressure a model footing can sustain, it seems reasonable to consider, instead of the pressure, a pressure parameter equal to the magnitude of the average pressure on the model footing divided by the unconfined compressive strength of the soil at the water content of the footing tests (σ/q_u). The dimensional analysis suggests that such a parameter should include some measure of soil strength, but it does not indicate what strength measure is most appropriate. The unconfined compressive strength is a useful quantity for two reasons: first, because the unconfined compression tests can be performed quite readily, and second, because the unconfined compressive strength represents the actual in-situ strength of the soil, thereby bypassing consideration of such complicating factors as stress history effects.

The utility of the pressure parameter is shown in Figure 4, in which the results of Figure 3 are replotted in terms of σ/q_u. The curves from Figure 3 are drawn much closer to each other in Figure 4. The scatter in this figure is felt to be due to the variation in water content which occurs within the soil bin for a given test series. There are two ways in which this variation can affect test results. First, zones of increased or decreased water content in the vicinity of the footing test result in a footing pressure, at a given penetration, which may be higher or lower than representative values for average conditions. Second, variability in the unconfined compression results is bound to occur as a result of inhomogeneity, water content variations, nonparallel ends of the test specimen, and other minor experimental difficulties which inevitably arise.

To improve the utility of the pressure parameter, an attempt has been made to correct in part for the variability in the unconfined compressive strength. Figure 5 shows the unconfined compressive strength determined for each test series plotted as a function of the average water content of the unconfined compression specimen. These points lie along a straight line on the semi-logarithmic plot within a range of water

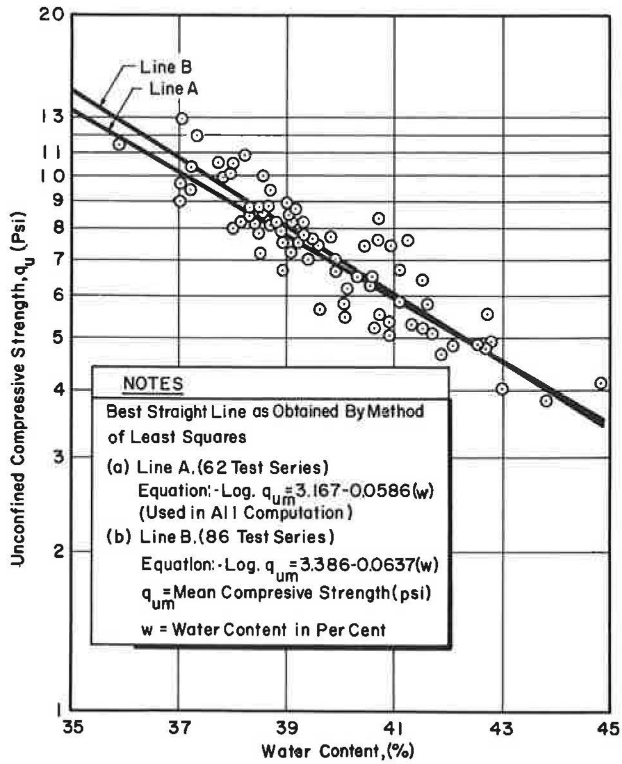

Figure 5. Water content vs unconfined compressive strength for EPK.

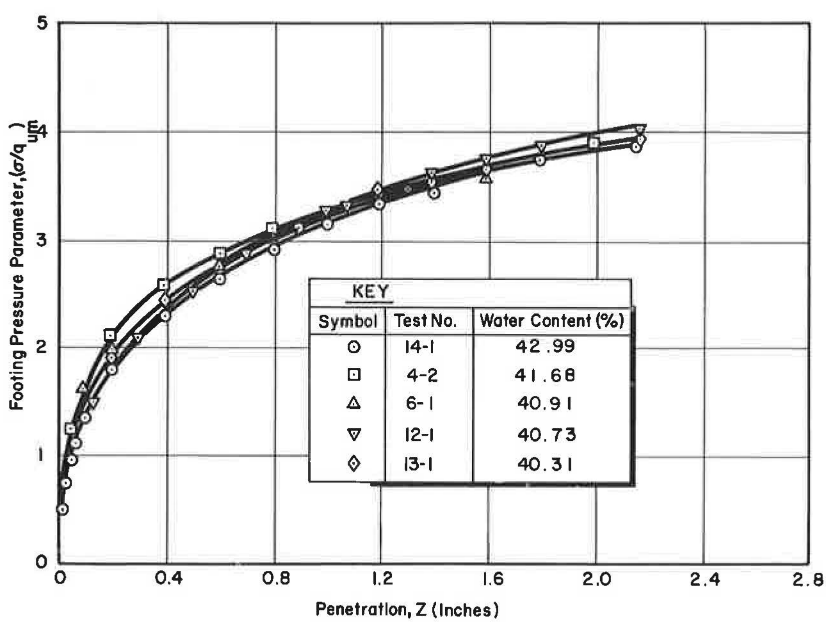

Figure 6. Effect of water content on pressure parameter-penetration relationship for 2-in. square footings on EPK.

contents from approximately 36 to 45 percent. The best straight-line fit of the plotted points (Fig. 5) was determined by the method of least squares. The value of the unconfined compressive strength indicated by this line at a particular water content is designated as the mean unconfined compressive strength, q_{um}. It appears that some experimental errors may be eliminated in the analysis by redefining the pressure parameter as the pressure on the model footing divided by the q_{um} corresponding to the water content of the soil. Figure 6 shows the data from Figures 3 and 4 with the footing pressure parameter recomputed as σ/q_{um}. Additional improvement can be noted in the approach of these data to a single curve, even though the unconfined compressive strength of the soil represented by these tests varies by a factor of approximately 1. 5.

The relationship shown in Figure 5 is also of use in preparing soils of a given consistency or strength. Utilizing this figure, it is possible to estimate quite closely the water content at which a given strength will be obtained.

Effect of Penetration Rate

Tests were performed at various rates of penetration to examine the effect of penetration rate on the pressure-penetration relationship. The tests were carried out at penetration rates from 0. 01 to 8. 0 cm/min on square, rectangular, and circular footings. Results of the tests on 2-in. square footings, which are typical of all the test data, are shown in Figure 7. These results indicate that, at large penetrations, the pressure parameter is substantially larger for the slowest test than for the fastest test. Also, at small penetrations the reverse is true. To interpret these results in a meaningful manner, it is perhaps useful to review a few well-established concepts about the influence of testing rate on the behavior of cohesive soils.

As noted previously, a model footing test on a cohesive soil is really only one of many possible forms of strength tests. Similarly, the pressure-penetration relationship is simply a type of stress-strain curve of the soil. Hence, insight into the effect of testing rate on the pressure-penetration relationship can be obtained by considering the ordinary stress-strain relationships obtained from laboratory strength tests. The influence of testing rate on the results of stress-strain tests on cohesive soils seems to be three-fold in nature:

1. The most significant effect of testing rate, by far, is to determine whether, and how much, drainage of pore fluid occurs during the course of the test. Drainage can be prevented by performing a test so rapidly that essentially no drainage occurs due to the relationship between the permeability of the soil and the speed of testing, or, in the case of strength tests in which a soil specimen can be completely enclosed, all

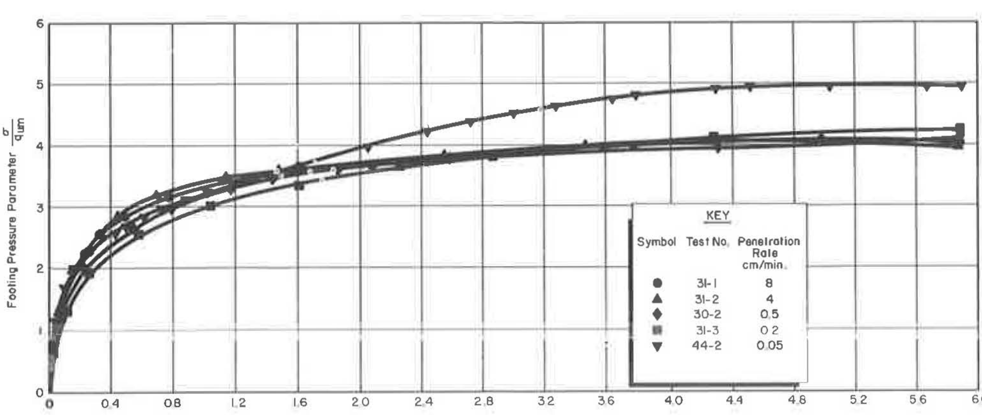

Figure 7. Effect of penetration rate on pressure-penetration relationship for 2-in. square footings on EPK.

drainage outlets are simply shut. If partial drainage occurs during loading, it may be difficult to compare test results.

2. Another important effect is that of soil creep (14, 18, 24). This effect is much more pronounced in some soils than others, and can be observed most strongly in sensitive and thixotropic soils. From the point of view of vehicle mobility, it hardly seems likely that stresses will be imposed on the soil at such a low rate that creep will become an important factor. Hence, it is important to perform the model footing tests in such a manner that creep is essentially eliminated. However, in the results shown in Figure 7 the soil appears strongest, at large penetrations, in the slowest test.

3. Finally, in general one must consider the dynamic, or inertial effect. Inertial effects occur only at very large testing rates, greatly in excess of those considered herein. Hence, dynamic effects can hardly be expected to be observed in the test results discussed.

Based on the foregoing discussion, it seems likely that the first two effects mentioned may be acting and influencing the curves shown in Figure 7. Indeed, this seems to be the case. Notice that at small penetrations, the slower tests lie below the faster tests. This would seem to be a minor manifestation of the creep effect. However, at large

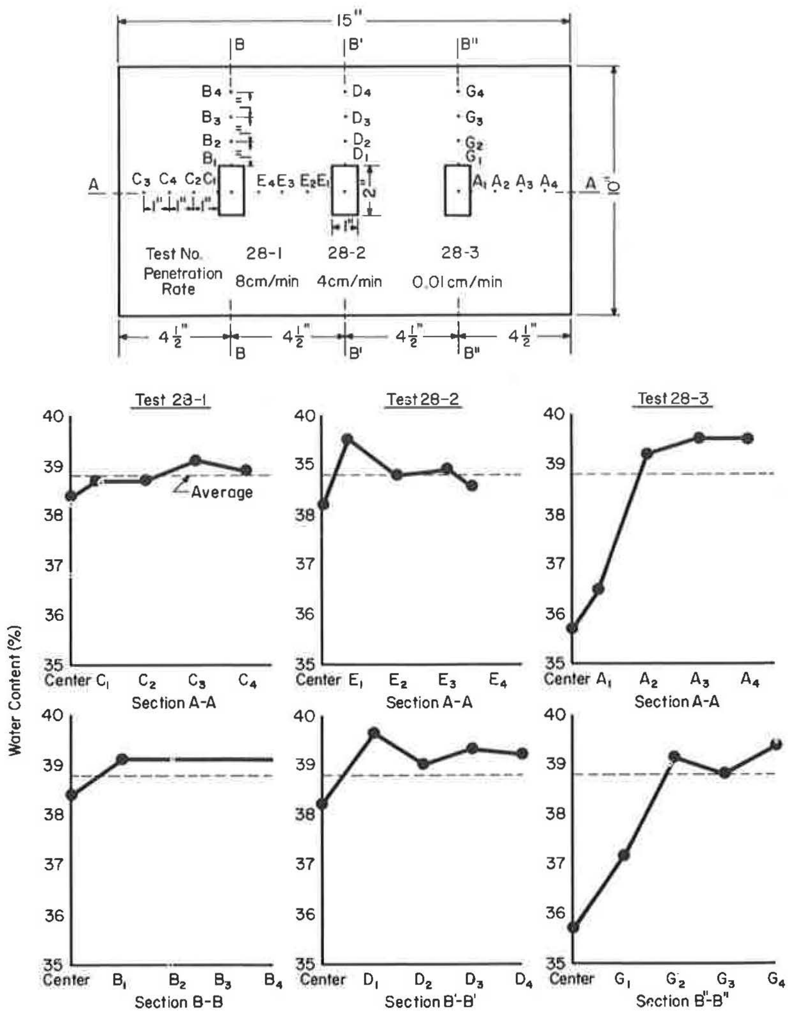

Figure 8. Effect of penetration rate on water migration under 1- by 2-in. model footings on EPK.

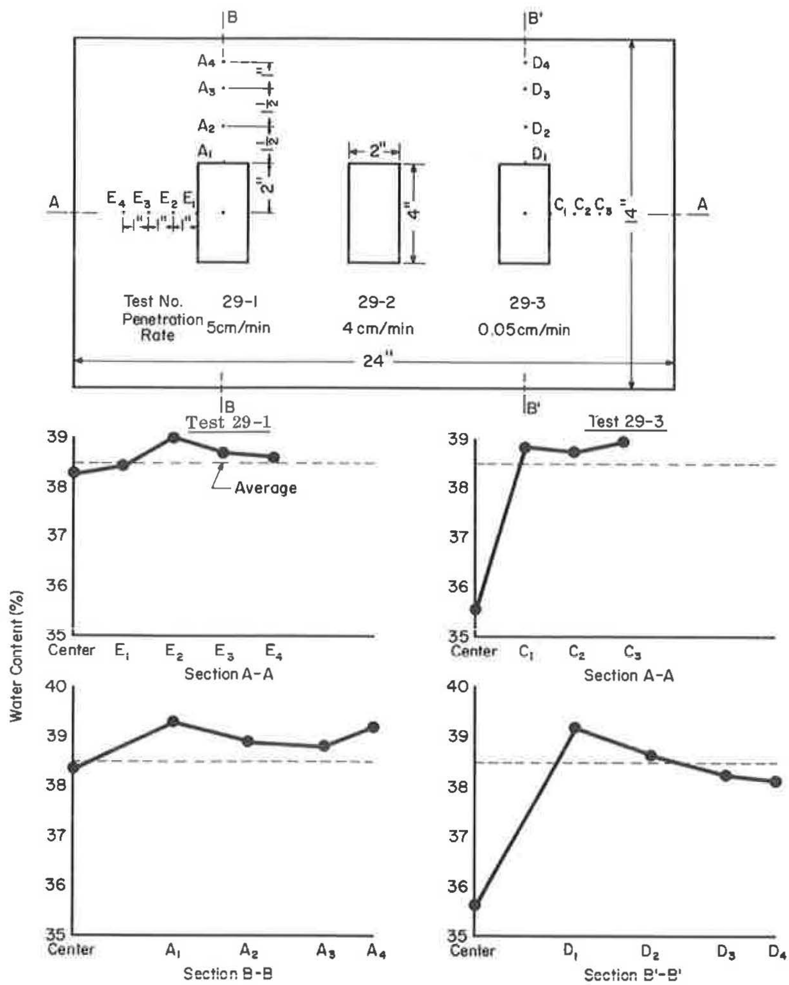

Figure 9. Effect of penetration rate on water migration under 2- by 4-in. model footings on EPK.

penetrations, and therefore, after longer times, the slower tests are stronger. This is probably due to migration of water away from the zones of high stress concentration underneath the footing permitted by the longer duration of the slower tests. If adequate time is provided for drainage to occur, the void ratio of the soil will decrease with a corresponding increase in strength.

The influence of penetration rate on moisture migration and the results for five model footing tests are shown in Figures 8 and 9. The locations of the model footings in the soil testing bins are shown in the upper part of the figures. At the completion of each test, the model footing was quickly removed and water content samples were taken from the elevation of the base of the footing at the locations shown in the upper part of the figures. The lower portions of Figures 8 and 9 show the variation in water content with distance from the center of each footing along the two principal axes. Several observations can be made about these results:

1. The water content immediately under the center of the footing is less than the average water content of the soil bin.
2. The loss in water content immediately under the center of the footing is quite clearly related to the rate of testing and/or the total time of testing. Thus in Figure 8,

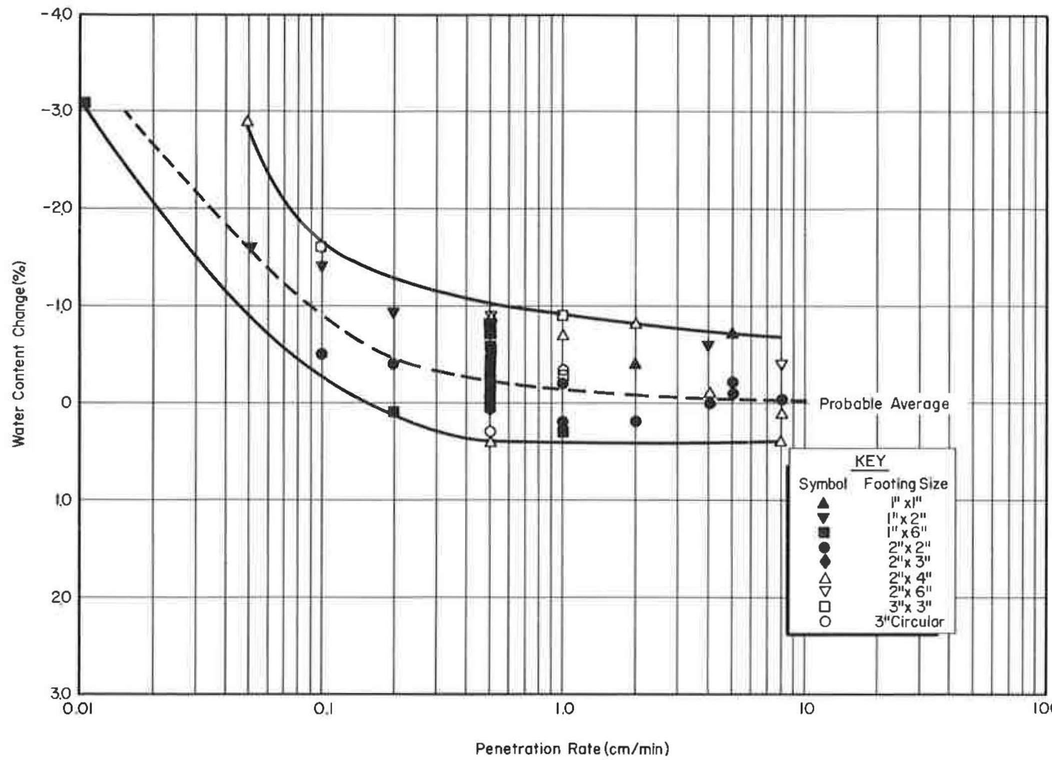

Figure 10. Effect of penetration rate on change in water content under model footing on EPK.

the water content under the center of the 1- by 2-in. footing tested at a penetration rate of 8 cm/min is only 0.4 percent below the average water content of the box; whereas for the test performed at a penetration rate of 0.01 cm/min, the water content under the center of the footing at the end of the test was 3.1 percent below the average water content of the soil mass. A similar result is shown in Figure 9. A quantitative measure of the effect of penetration rate on moisture migration is shown in Figure 10. The figure shows the difference in water content between a point immediately under the center of the footings and the average for the soil bin, plotted as a function of the penetration rate. There are some points at the higher penetration rates for which there is actually a slight increase in water content under the footing. This is undoubtedly due to the unavoidable small nonuniformities which always occur. However, the average results of many tests show that the water content under the footing is essentially unchanged, as the penetration rate varies from 8 cm/min to approximately 0.5 cm/min, and decreases sharply at lower penetration rates. It is important to remember, however, that the results obtained by measuring the water content immediately under the footing, and at points at the elevation of the base of the footing, will indicate changes in water content much larger than probably exist at some depth below the footing. Inasmuch as the pressure required to produce a given penetration depends on the resistance of the soil within a large zone under the footing, the results in Figures 8 and 10 indicate a limiting condition only, and not a result typical of this entire zone. Hence, it may be concluded from Figures 7 and 10 that penetration rates of the order of 0.5 cm/min, and greater, are adequately high to prevent artifacts in the experimental results due to moisture migration underneath the footing.

3. In almost all cases the water content just outside the edge of the footing is higher than the average for the entire box. A theoretical analysis for a footing embedded within an elastic medium (21) shows that in the vicinity of the edge of the footing, tension

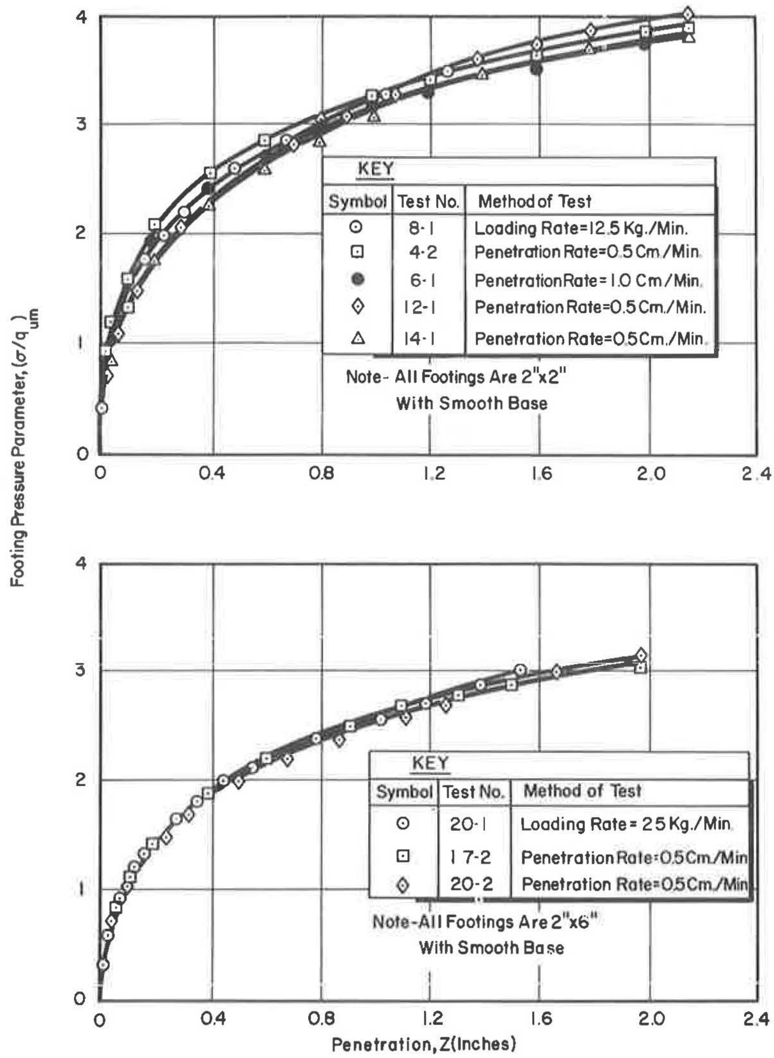

Figure 11. Effect of test method on pressure parameter-penetration relationship for EPK.

exists in the medium. In a cohesive soil, the tensile stress causes migration of pore water from the compressive zone immediately under the footing, and the relatively unstressed material outside the footing, into the zone which is in tension.

Effect of Type of Testing

The pressure-penetration relationship from model footing tests on cohesive soils will eventually be applied to the prediction of vehicle sinkage in similar soils. A vehicle imposes a load on the soil with penetration occurring as a function of the load. Therefore, it would seem appropriate to perform the model footing test with the same type of loading. However, it is experimentally simpler to use a constant rate of penetration method. Hence, the constant penetration rate type of test was compared with a constant loading rate type of test to determine whether the two tests are truly equivalent. Figure 11 shows the results of two such comparisons made on square and rectangular footings. These results indicate that the two types of tests produce virtually identical effects.

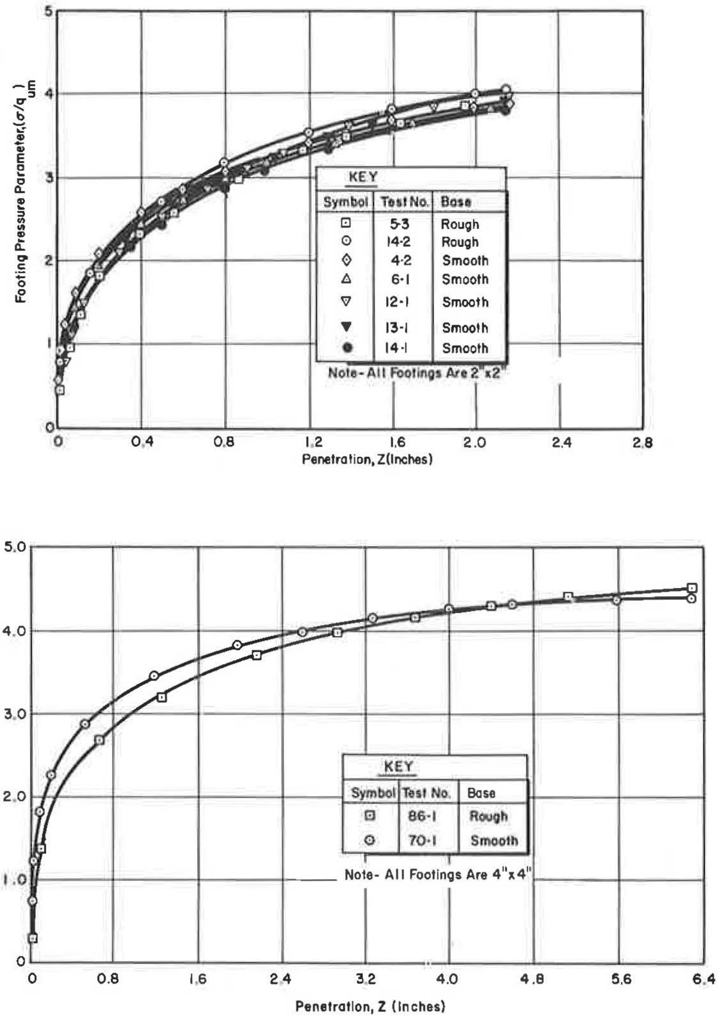

Figure 12. Effect of base roughness on pressure parameter-penetration relationship for square footings on EPK.

This result seems reasonable when the mechanism of constant rate of loading tests is considered. To carry out such tests, it is necessary to vary the penetration rate continuously to insure that the loading rate remains constant. Hence, at small penetrations the penetration rate required to maintain a constant loading rate is very small, whereas at large magnitudes of penetration, the penetration rate required is much higher. This is indicated in Table 2 which gives data from one test performed at a constant rate of loading on a 2-in. square footing. The penetration rate required to maintain a constant loading rate at the end of the test is approximately 50 times that required to maintain the same loading rate at the beginning of the test.

Therefore, the effect of test type is really quite similar to the effect of varying the rate of penetration, and the comments in the preceding section apply here as well. Thus, it seems that the type of testing does not influence results as long as the average rate of penetration is sufficiently high to prevent significant drainage of water from the zone beneath the footing.

TABLE 2

PENETRATION RATES DURING CONSTANT RATE OF LOADING TEST[a]

Load Interval (kg)	Avg. Penetr. Rate During Load Interval (cm/min)	Ratio of Penetr. Rate to Initial Penetr. Rate
0-2.5	0.075	1
10-12.5	0.275	3.7
20-22.5	1.09	14.5
30-32.5	2.46	32.8
35-37.5	3.83	51.1

[a]Test number: 8-1; 2-in. square smooth base footing; rate of loading: 12.5 kg/min.

Effect of Roughness of Footing Base

Theoretical analyses of the ultimate bearing capacity of purely plastic material being penetrated by a rigid punch indicate that a punch with a "perfectly rough" base will be capable of sustaining a pressure approximately 10 to 30 percent larger than a punch with a "perfectly smooth" base (15, 27) depending on the shape of the punch. Thus, it becomes important to determine what effect the condition of the base of the model footings will have on experimental results. Consequently, comparative tests were performed for a variety of footing sizes on "smooth" and "rough" base footings. The smooth base footings had polished sides and bases, and were lubricated with silicone fluid on all surfaces in contact with the soil. The rough base footings had polished sides, but the bases were roughened, as previously described. The sides were lubricated with silicone fluid, but the base was not. The results of such

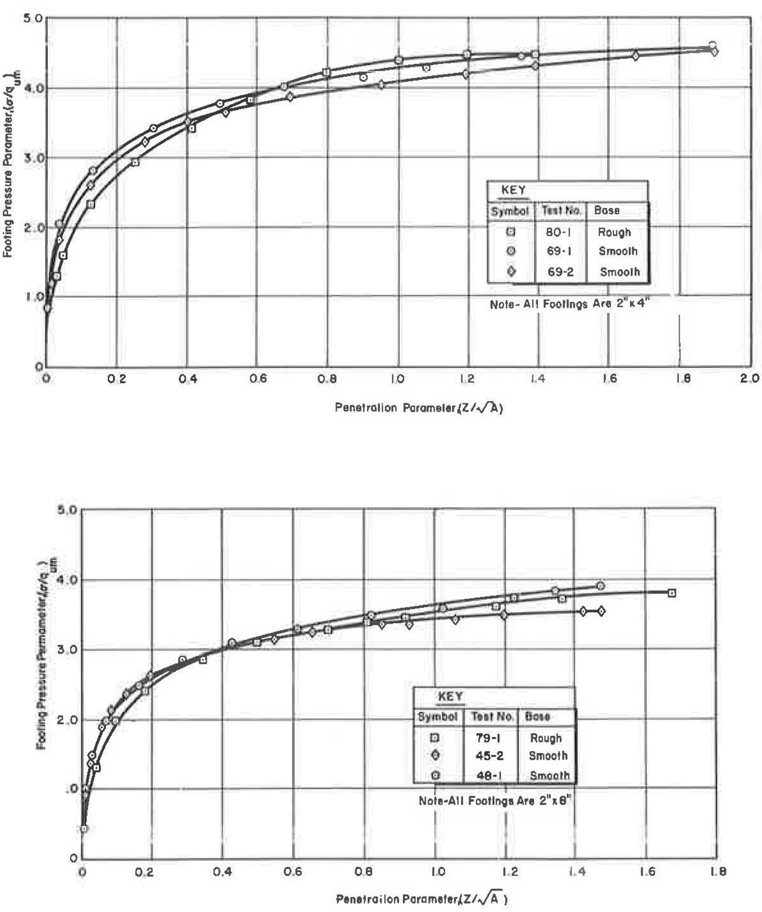

Figure 13. Effect of base roughness on pressure parameter-penetration relationship for rectangular footings on EPK.

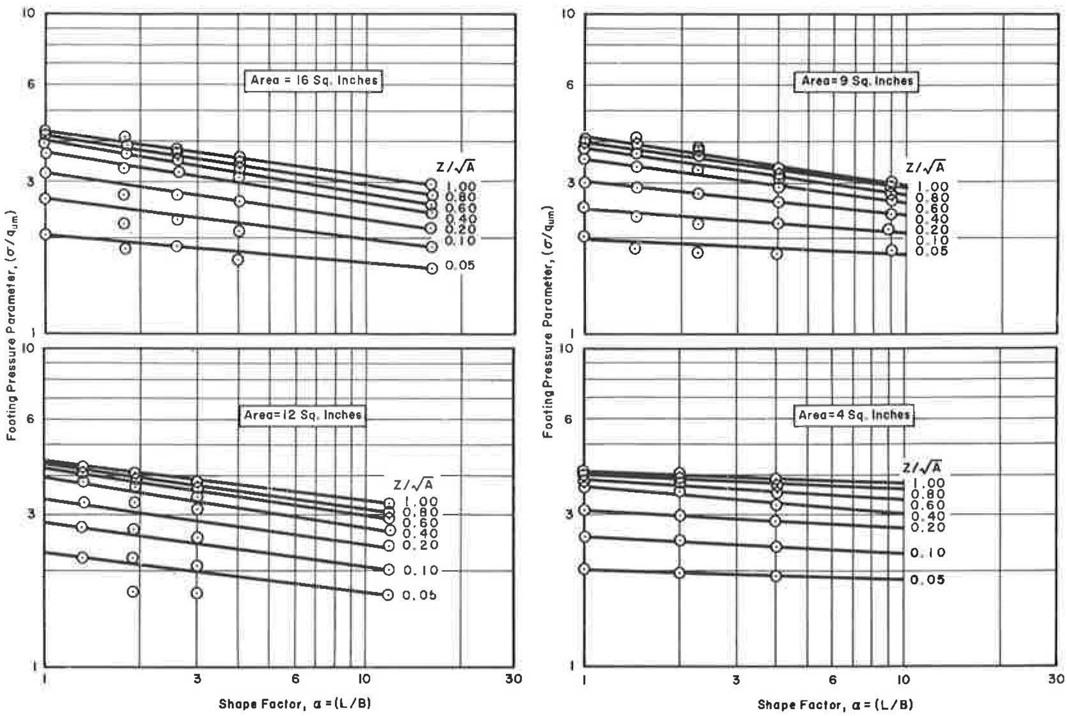

Figure 14. Effect of shape factor on pressure parameter for constant area footings on EPK.

comparative tests for square and rectangular model footings are shown in Figures 12 and 13. Surprisingly, these results suggest no effect of footing roughness on the pressure-penetration relationship. The reason for this appears to lie in the definition of "smooth base" and "rough base." In the theoretical analyses, a smooth base punch is mathematically characterized by the fact that no shear stress exists at the punch-soil interface. Similarly, the rough base punch is characterized by the fact that no relative horizontal displacement occurs between the punch and the soil at the punch-soil interface. Observation of the soil distortion underneath a footing after the removal of the footing at the end of a test suggests that even for the lubricated, so-called smooth base footings, some friction actually does develop due to the large normal pressures at the base of the footing. Hence, although a polished lubricated footing feels smooth to the touch, when it is pressed into the soil, its behavior can be characterized by the mathematical definition of a rough footing. Thus, for practical purposes, it appears impossible to prepare a model footing sufficiently smooth to prevent the development of shear stress between the footing and the soil.

Because it is simpler to prepare polished footings, the majority of the footings were constructed with polished surfaces.

PRESSURE-PENETRATION RELATIONSHIP

The previous sections have considered, and accounted for, a variety of factors which might influence the pressure-penetration relationship and obscure size and shape effects. After extraneous factors were eliminated, an examination of available pressure-penetration equations (1, 2, 5, 6, 11) was made. None of the suggested relationships was found to represent reasonably the data obtained in this study, or the published data of other investigators for a wide range of penetrations. Hence, a more meaningful relationship was sought.

The approach taken was to establish an empirical description of the pressure-penetration relationship, utilizing the observed relationship itself. When the various factors discussed in the preceding sections are held constant, the dimensional analysis suggests that the pressure should be a function of penetration, size, and shape of the model footing. A theoretical analysis by Schleicher (23) shows that penetration can be most appropriately represented in a dimensionless form by a penetration parameter, $z/\sqrt{A}$, and the shape effect can be represented by the ratio of length to width, L/B (herein designated α).

To elucidate the influence of shape, a number of model footing tests were carried out on footings of constant area with varying shape factors. Figure 14 shows the results of such tests for areas of 4, 9, 12, and 16 sq in. These results are shown in the form of footing pressure parameter plotted as a function of the shape factor, to logarithmic scales, for given values of penetration parameter. Except for very small values of penetration for the smaller footings, the slopes of these lines on logarithmic scales are approximately constant (Fig. 15). This figure shows the logarithmic slopes of these lines as a function of $z/\sqrt{A}$. Although there is considerable scatter apparent in Figure 15, the actual variation in slope of the lines in Figure 14 is not so large. It is not clear from Figure 15 whether or not there is a significant effect of area on these slopes. However, data for another soil, given below, suggest that, in fact, the slopes of the lines in Figure 14 are independent of area. Hence, it will be assumed here that the shape effect is independent of footing area and the magnitude of penetration.

The equation of these lines can be written as

$$\sigma/q_u = F\ (z/\sqrt{A})\ \alpha^{-D} \tag{3}$$

where $F\ (z/\sqrt{A})$ is the pressure corresponding to a given penetration for a square or circular footing (for which $\alpha = 1$) and D is the average absolute value of the logarithmic slopes of the lines in Figure 14. Eq. 3 states that, for a given size footing, the resistance to penetration decreases as the ratio of length to width increases. This result is in agreement with standard bearing capacity analyses for cohesive soils (26, 27). In fact, the numerical values of the shape effect term, α^{-D}, are close to those found experimentally by Meyerhof (15) for the effect of shape on the bearing capacity of model footings in clay.

The quantity $F\ (z/\sqrt{A})$ is actually the pressure-penetration relationship for square and circular footings, for which $\alpha = 1$. The relationship is shown in Figure 16 for 19 tests on square and circular footings with areas varying from 4 to 16 sq in. The penetration is represented by the penetration parameter, $z/\sqrt{A}$. The mean curve for all the tests is indicated by the dashed line. Examination of the plotted points shows that the scatter from the mean curve does not follow any consistent pattern, and can probably be attributed to the unavoidable variability always present in experimental results. Thus, the parameter $z/\sqrt{A}$ appears significant, because the pressure-penetration relationships for all of these square and circular footings reduce to the same curve when penetration is represented by this penetration parameter.

A variety of expressions by which the relationship shown in Figure 16 could be represented has been studied, and the two-constant rectangular hyperbola shown below appears to be the most applicable:

$$\sigma/q_u = \frac{z/\sqrt{A}}{M + Q\ z/\sqrt{A}} \tag{4}$$

where M and Q are constants.

To determine if the pressure-penetration relationships shown in Figure 16 can reasonably be represented by Eq. 4, a test plot can be constructed (8). Eq. 4 can be rewritten as

$$\frac{z/\sqrt{A}}{\sigma/q_u} = M + Q\ z/\sqrt{A} \tag{5}$$

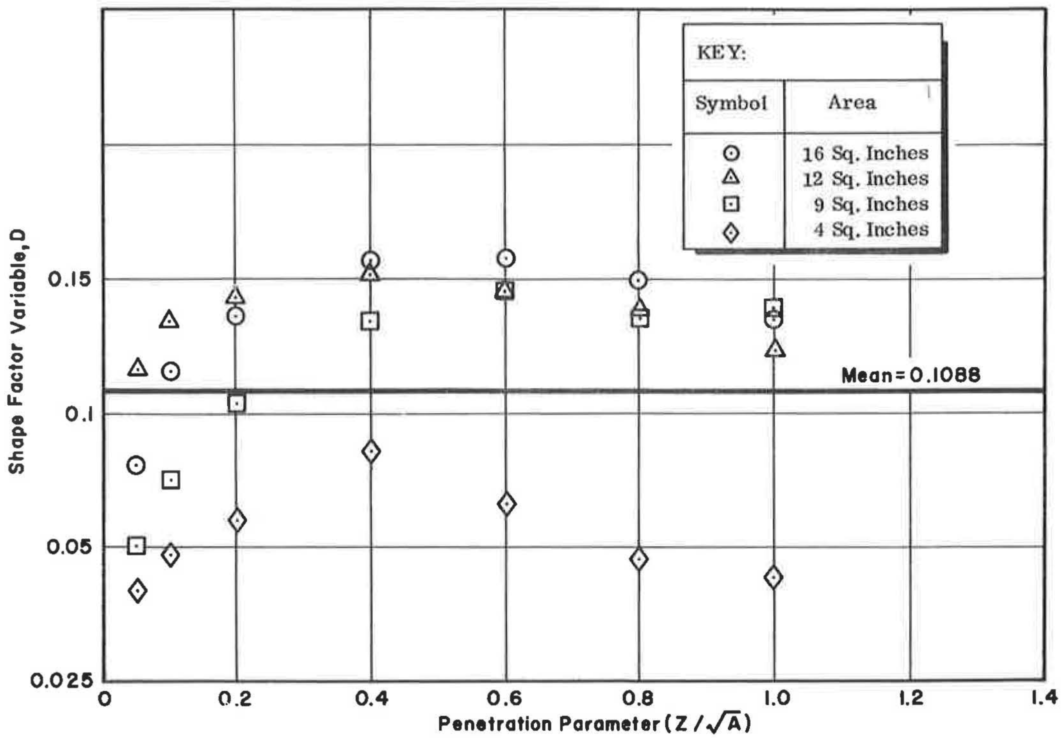

Figure 15. Effect of footing area and penetration on logarithmic slope of lines in Figure 14.

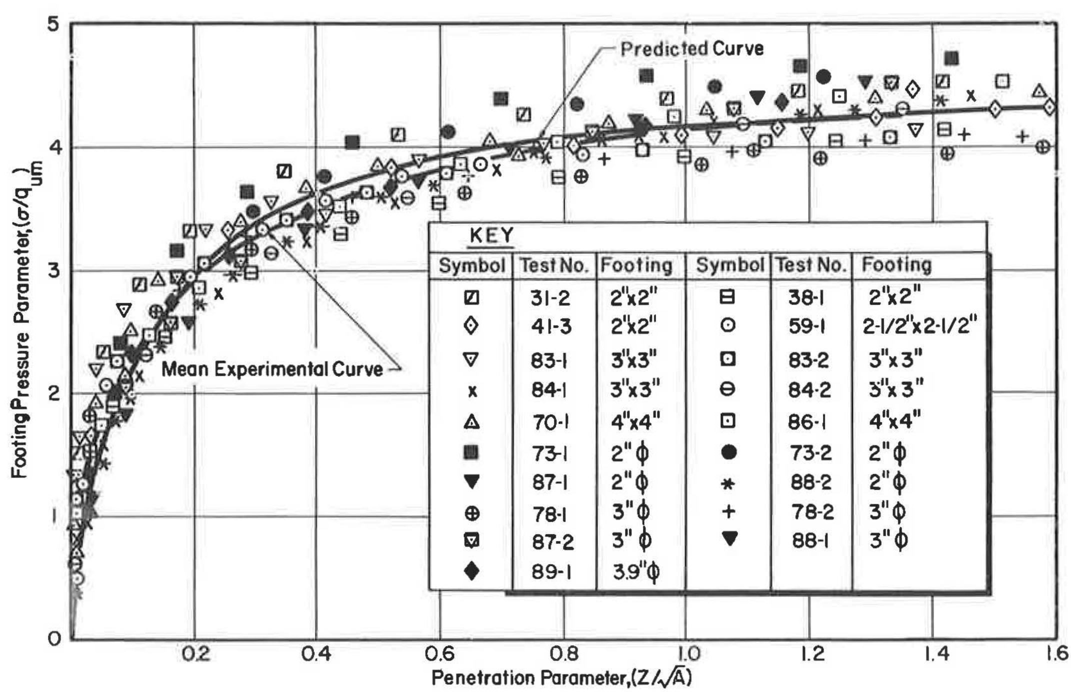

Figure 16. Pressure-penetration relationship for square and circular footings on EPK ($\alpha = 1$).

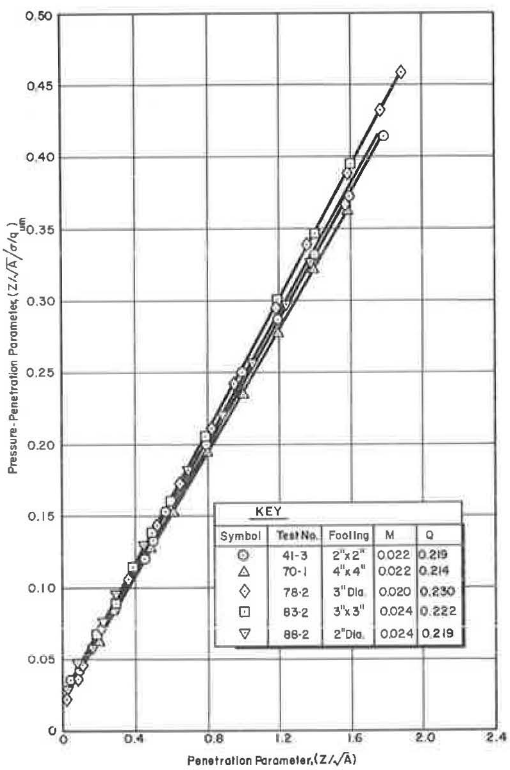

Figure 17. Hyperbolic pressure-penetration test plots for square and circular footings on EPK.

which is the equation of a straight line. Hence, if the data in Figure 16 can, in fact, be represented by Eq. 4, these data will appear as a straight line when plotted in the form of Eq. 5.

The typical test plots of this sort in Figure 17 show that Eq. 4 does satisfactorily represent the experimental data over a large range of penetrations. The constants in Eq. 4 are determined from the test plot: M is the σ/q_u intercept when $z/\sqrt{A} = 0$, and Q is the slope of the test plot line.

A physical interpretation can be ascribed to the constants M and Q in Eq. 4. By the appropriate substitutions it can be seen that 1/M is the initial tangent modulus (slope) of the hyperbolic curve. The quantity 1/Q is the magnitude of the pressure parameter to which the hyperbolic curve is asymptotic.

The test plot lines in Figure 17 all lie quite close to each other, and it is not surprising that the magnitudes of the constants M and Q are all quite close. The fact that there is no significant influence of area on the magnitude of these constants is shown by Figure 18, in which the constants M and Q have been plotted as a function of $1/\sqrt{A}$. Although some experimental scatter is present, there does not appear to be any consistent trend as a function of footing area.

Combining Eqs. 3 and 4 results in an empirical pressure-penetration relationship which should predict the behavior of model footings of various shapes and sizes:

$$\sigma/q_u = \frac{z/\sqrt{A}}{M + Q\, z/\sqrt{A}}\, \alpha^{-D} \tag{6}$$

where D = 0. 1088, M = 0. 0232, and Q = 0. 219 for the cohesive soil (EPK) tested. Eq. 6 predicts that the relationship between σ/q_u and $z/\sqrt{A}$ for square and circular footings is unique for all size footings, and that the shape effect is independent of footing size.

The validity with which Eq. 6 represents the actual pressure-penetration data for model footings on EPK is shown in Figures 16 and 19 through 24. These figures show results for square, circular, rectangular, and elliptical footings with areas from 2 to 27 sq in. and length-to-width ratios from 1 to 16. The results of tests on square and circular footings of various sizes are shown in Figure 16. The solid line is the predicted curve, and inasmuch as it was determined essentially from these same points, it is not surprising that the predicted curve represents the data quite well. The results for both squares and circles ($\alpha = 1$) are indistinguishable from each other. Similar comparisons are made for values of α greater than one, and a variety of areas (Figs. 19-24). As the constants in the hyperbolic expression were determined from the data for square and circular footings (Fig. 16), the excellent representation of the data by the prediction equation is considered a demonstration of the validity of this approach.

Figures 20 and 21 show the results of tests on elliptical footings. It seems clear that rectangular and elliptical footings yield essentially the same results (which can be represented by the prediction equation) when the rectangle and ellipse being compared

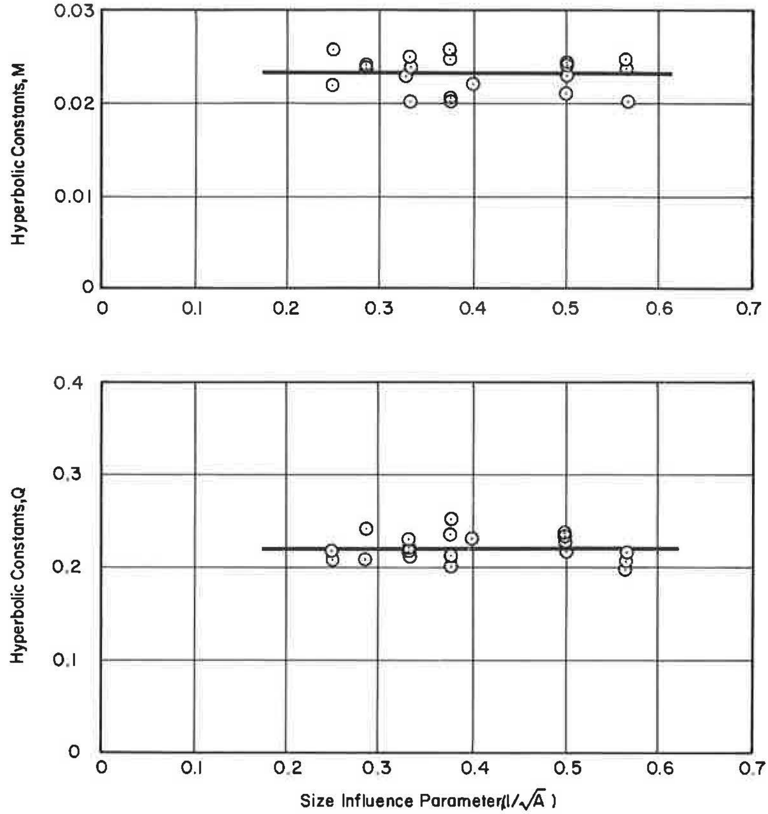

Figure 18. Relationship between the hyperbolic constants M and Q and footing area for EPK.

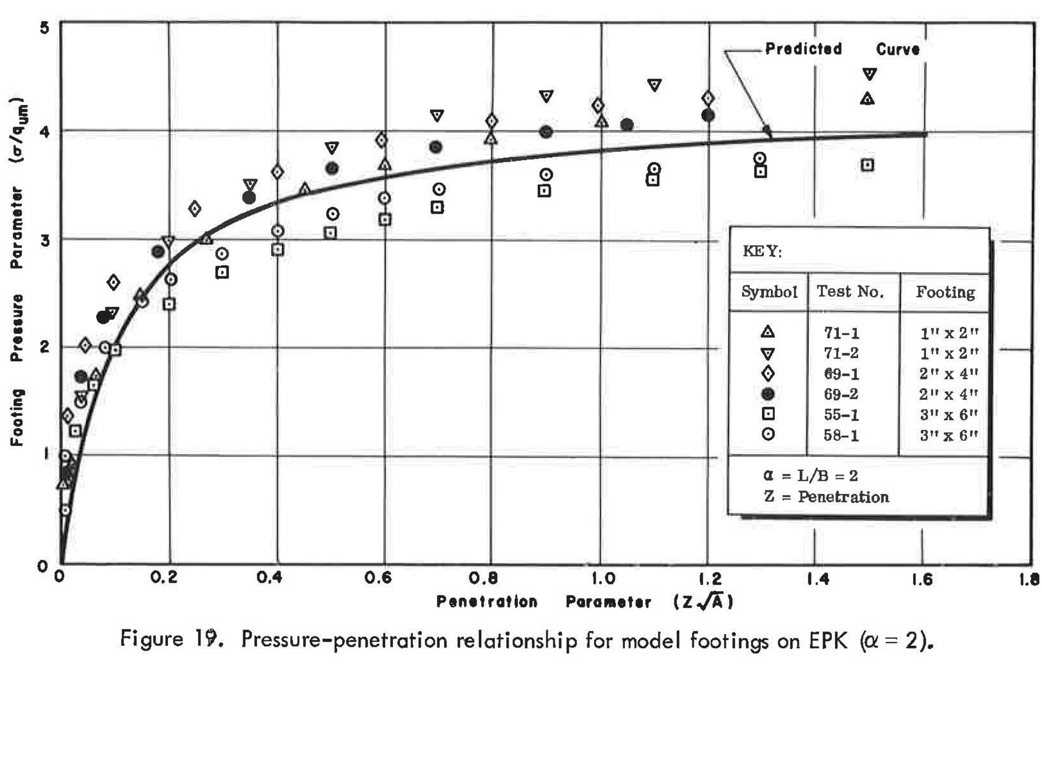

Figure 19. Pressure-penetration relationship for model footings on EPK ($\alpha = 2$).

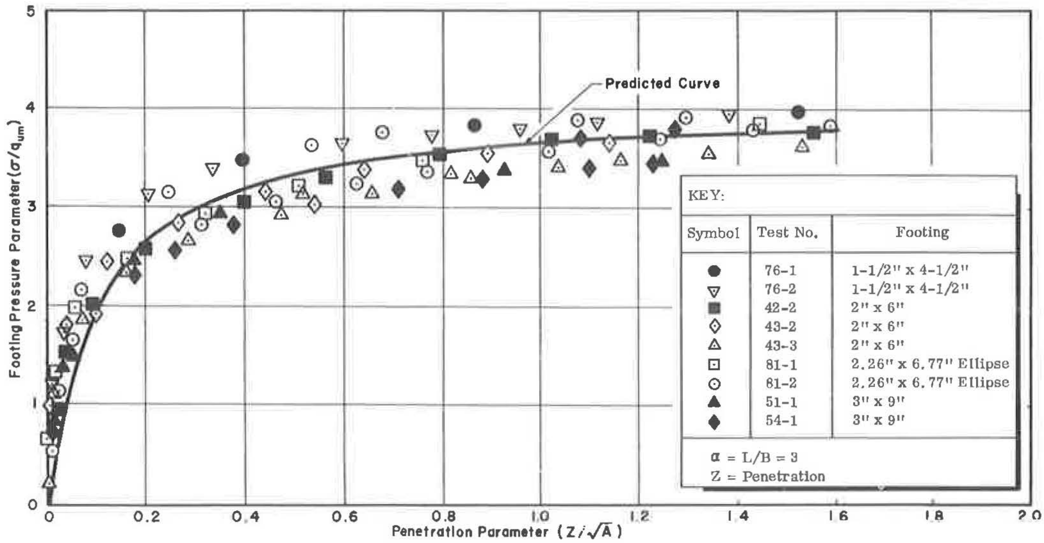

Figure 20. Pressure-penetration relationship for model footings on EPK ($\alpha = 3$).

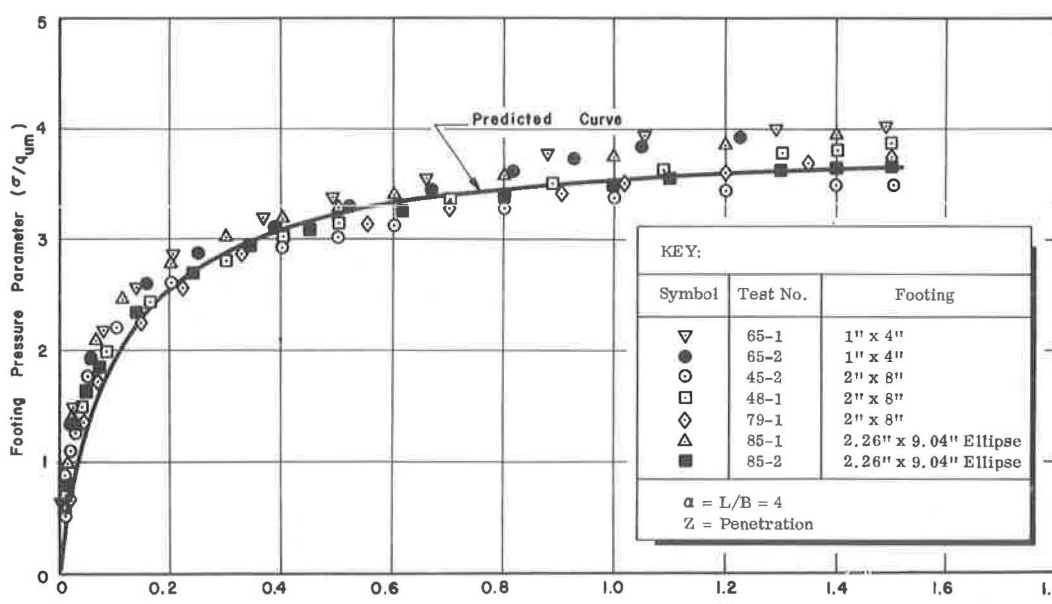

Figure 21. Pressure-penetration relationship for model footings on EPK ($\alpha = 4$).

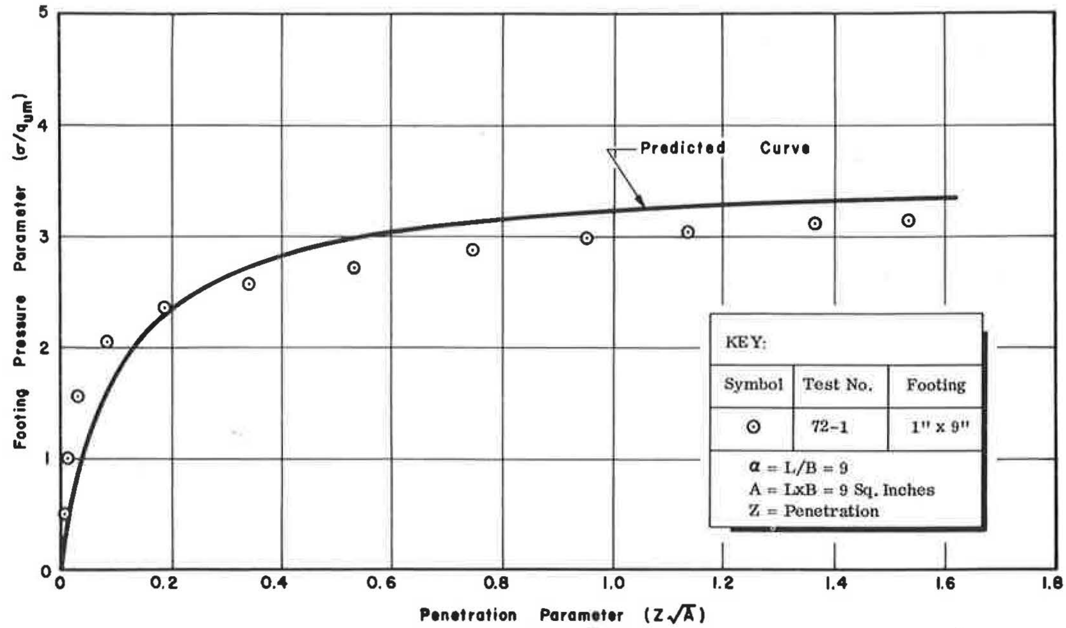

Figure 22. Pressure-penetration relationship for model footings on EPK ($\alpha = 9$).

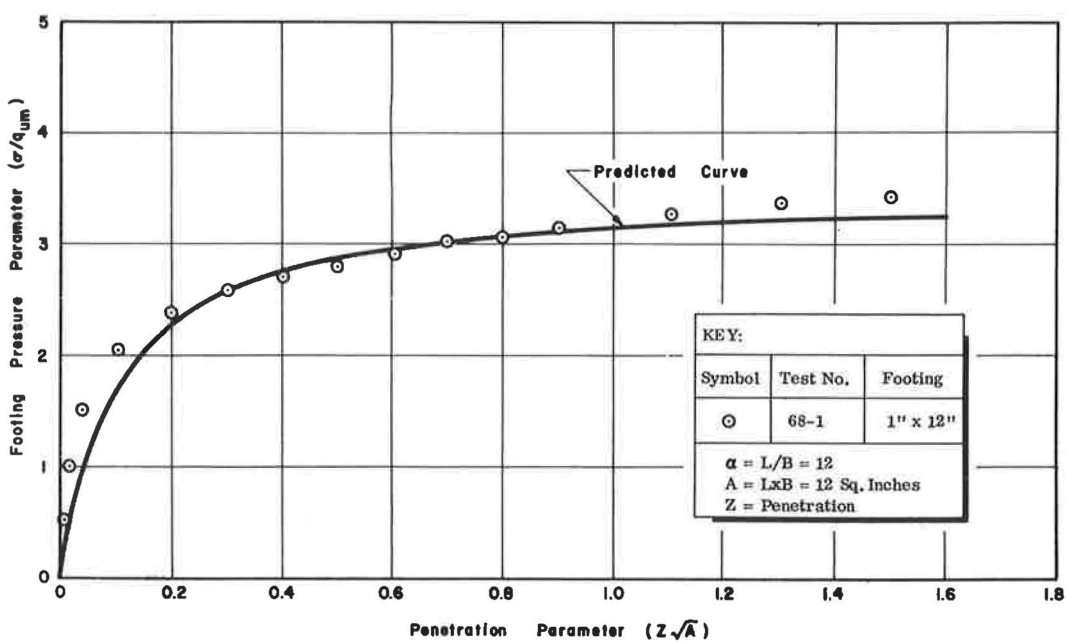

Figure 23. Pressure-penetration relationship for model footings on EPK ($\alpha = 12$).

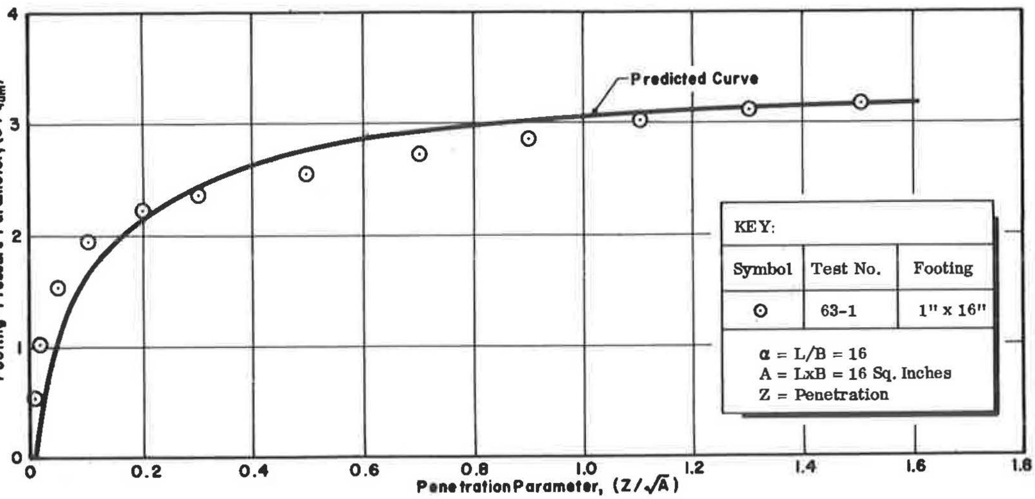

Figure 24. Pressure-penetration relationship for model footings on EPK (α = 16).

have the same area and the same α. In the case of the ellipse, α is also considered to be the length-to-width ratio, i.e., the ratio of the length of the major and the minor axes. For example, Figure 20 shows results for rectangles and ellipses of 12 sq in. in area, with $\alpha = 3$. In this case, the rectangles were 2 in. wide by 6 in. long, and the minor and major axes of the ellipses were 2. 26 in. and 6. 77 in., respectively.

A similar series of tests was performed on a mined soil from Goose Lake County, Ill. The soil, called Grundite, is sold in dry powdered form, and is primarily an illite with approximately 15 percent fine quartz. Classification properties of Grundite are

Liquid limit: 55. 6 percent
Plastic limit: 32. 0 percent
Plasticity index: 23. 6 percent
Specific gravity of solids: 2. 84
Clay size fraction (<0. 002 mm): 64 percent

The results of the tests on saturated Grundite are shown in Figures 25 through 35. Figures 25 and 26, for Grundite, are analogous to Figures 14 and 15 for EPK. They further suggest that the shape effect is essentially independent of the magnitude of penetration and the footing area. Figure 27 shows the results for square and circular footings ($\alpha = 1$). Again, the scatter is no more than can be expected from experimental results. The test plots for Eq. 4 are given in Figure 28 for several of the experimental curves. The agreement over a wide range of penetrations is evident, both in Figure 28 and in Figure 27 where Eq. 4, with the appropriate constants inserted, is shown. Figure 29 shows that the constants M and Q for Grundite, as for EPK, are not significantly affected by footing area.

Figures 30 through 35 show the results for footings on Grundite with α ranging from 1. 77 to 16. The reliability of Eq. 6 is somewhat less for the Grundite than for the EPK (Figs. 19-24). This appears to be primarily due to the influence of the tests on the 4-sq in. footings (Fig. 26). Certainly the predicted curves are valid within expected experimental error.

Kondner and Krizek (11) have also suggested a two-constant hyperbolic expression for the pressure-penetration relationship. However, the similarity appears superficial, because they examined only penetrations of very small magnitude, and utilized a penetration parameter somewhat different from that considered herein. In addition, their test results for very small scale model footings (2 sq in. in area) indicate that as the ratio of length to width increases, the footing pressure required for a given penetration

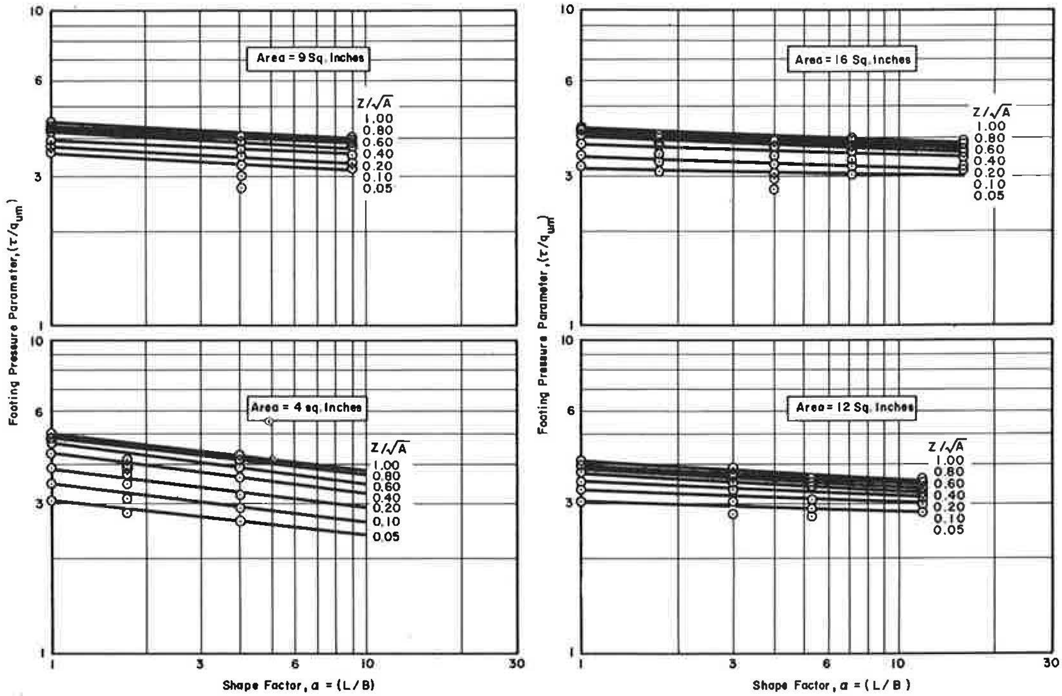

Figure 25. Effect of shape factor on pressure parameter for constant area footings on Grundite.

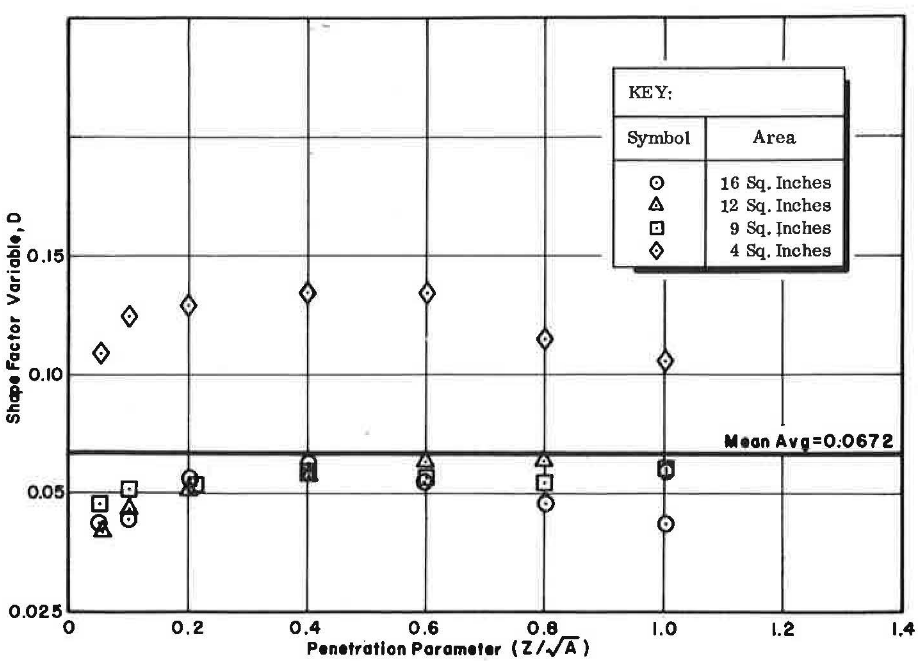

Figure 26. Effect of footing area and penetration on logarithmic slope of lines in Figure 25.

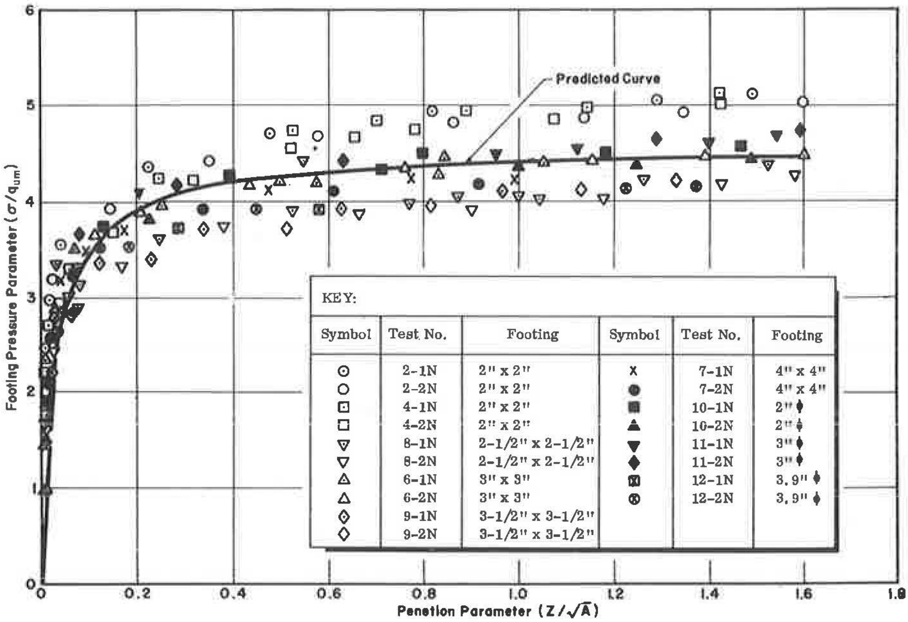

Figure 27. Pressure-penetration relationship for square and circular footings on Grundite ($\alpha = 1$).

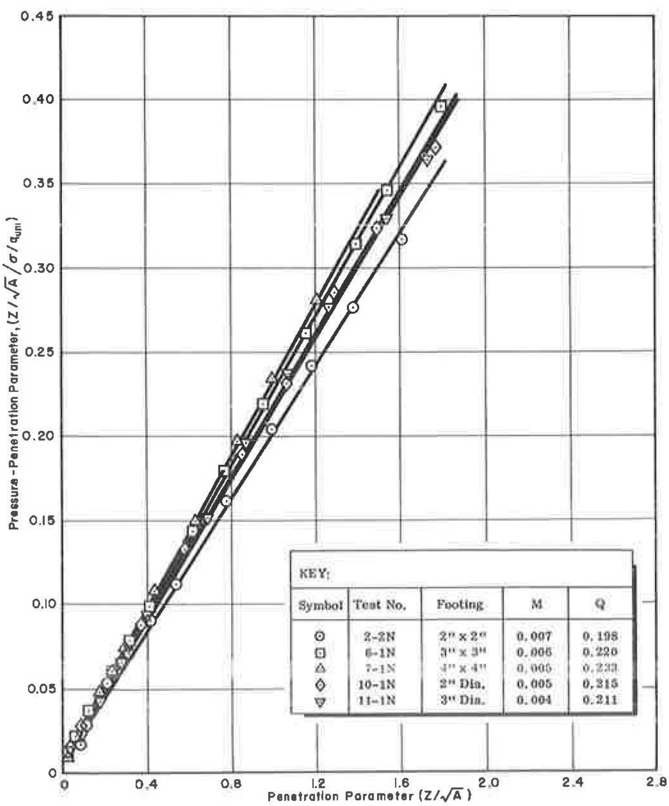

Figure 28. Hyperbolic pressure-penetration test plots for square and circular footings on Grundite.

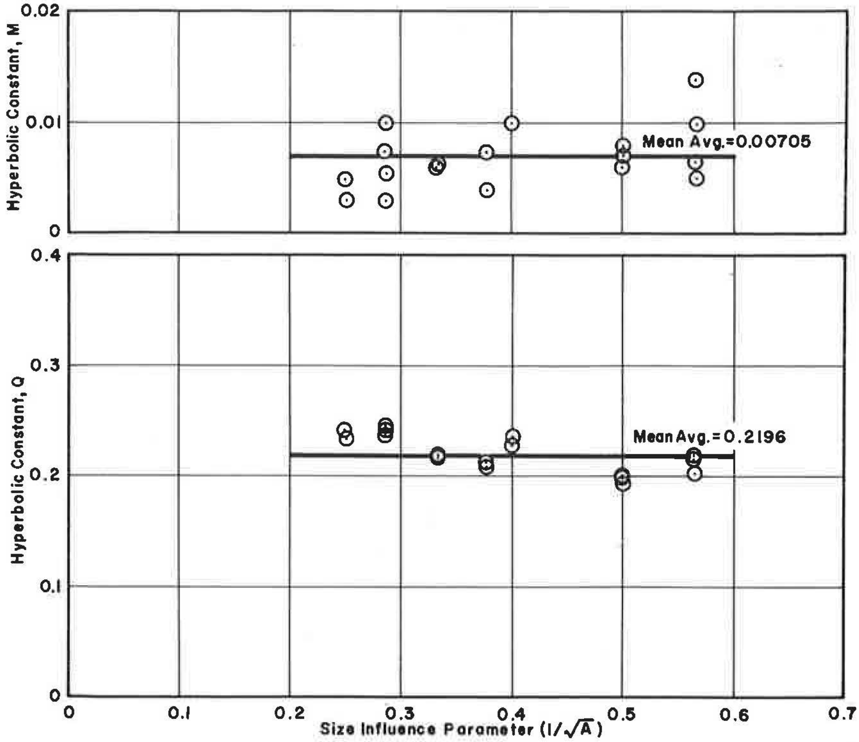

Figure 29. Relationship between hyperbolic constants M and Q and footing area for Grundite.

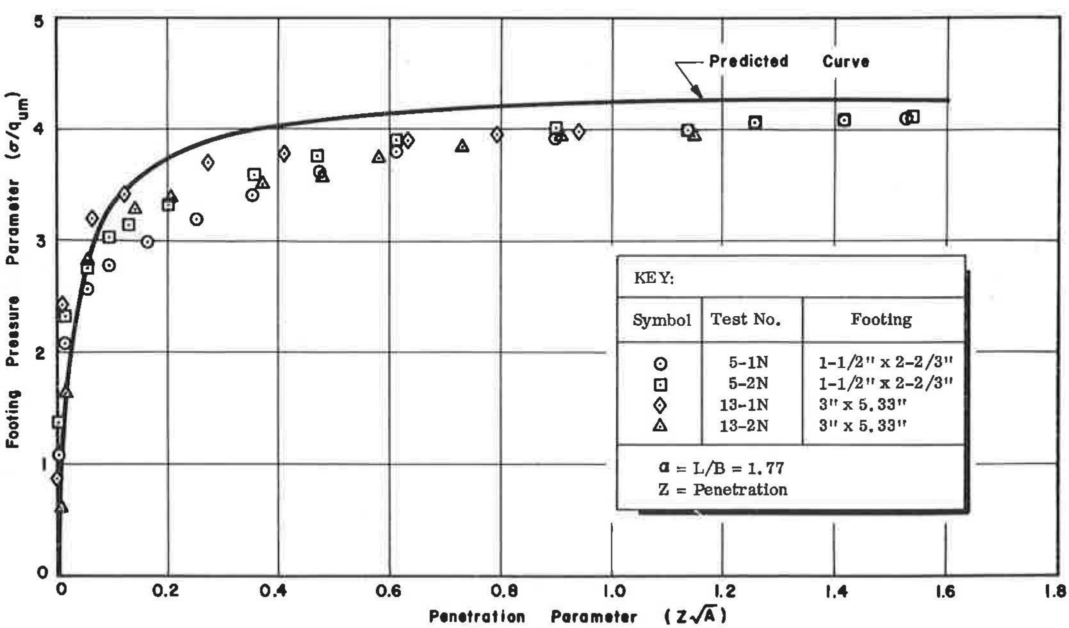

Figure 30. Pressure-penetration relationship for model footings on Grundite (α = 1.77).

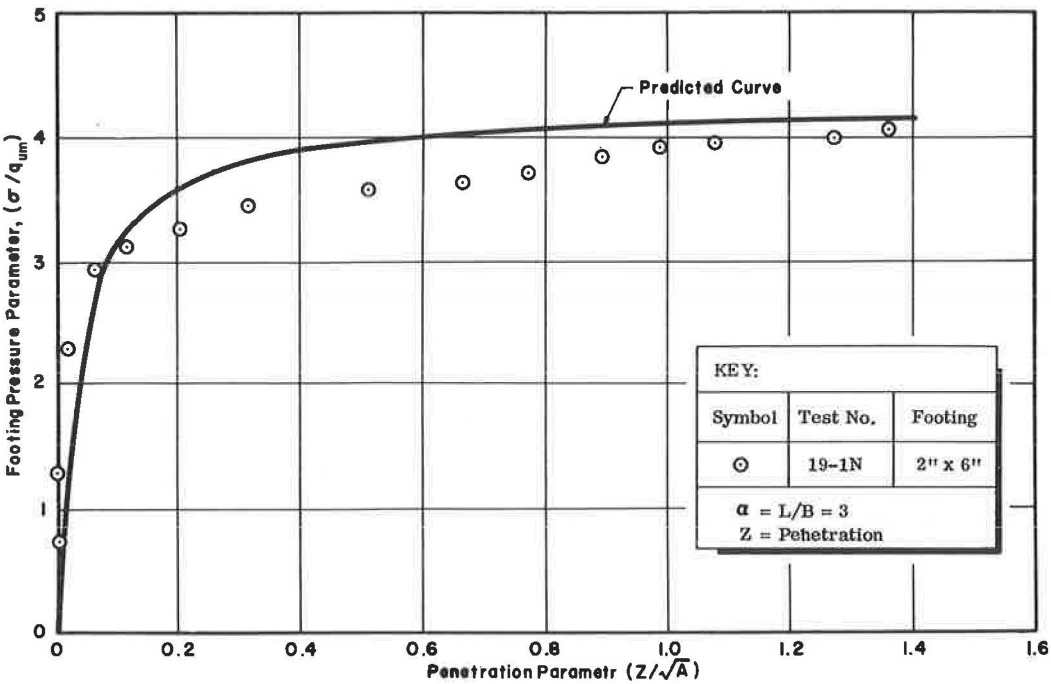

Figure 31. Pressure-penetration relationship for model footings on Grundite (α = 3).

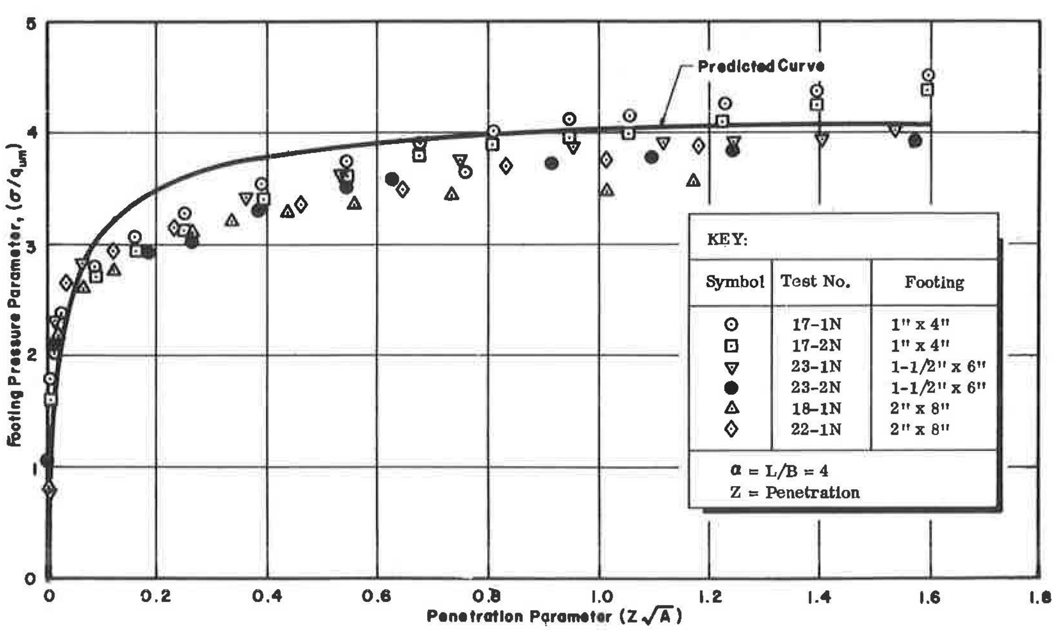

Figure 32. Pressure-penetration relationship for model footings on Grundite (α = 4).

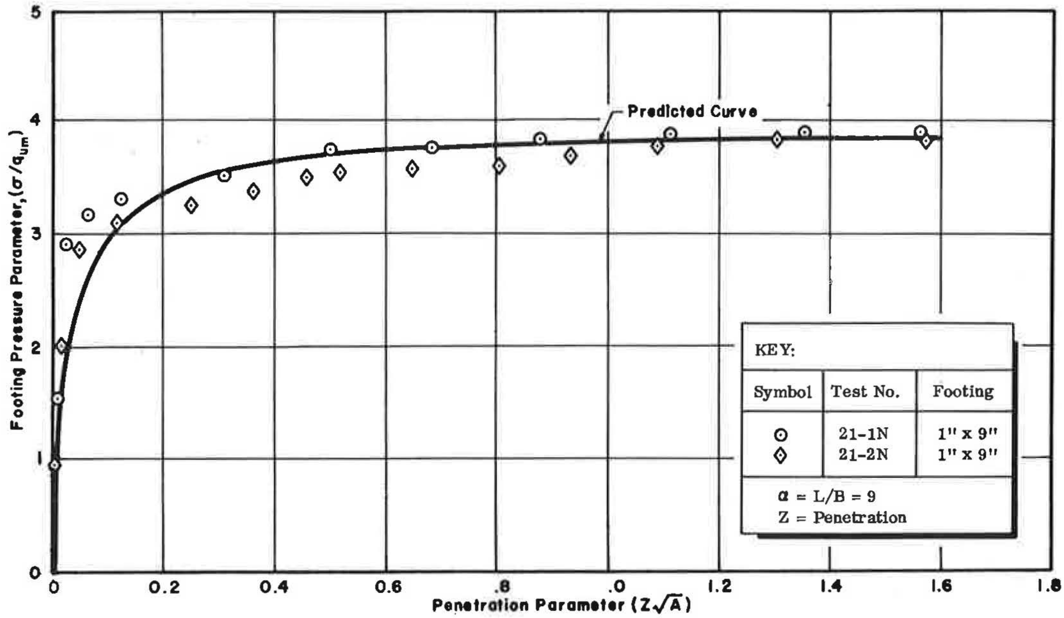

Figure 33. Pressure-penetration relationship for model footings on Grundite (α = 9).

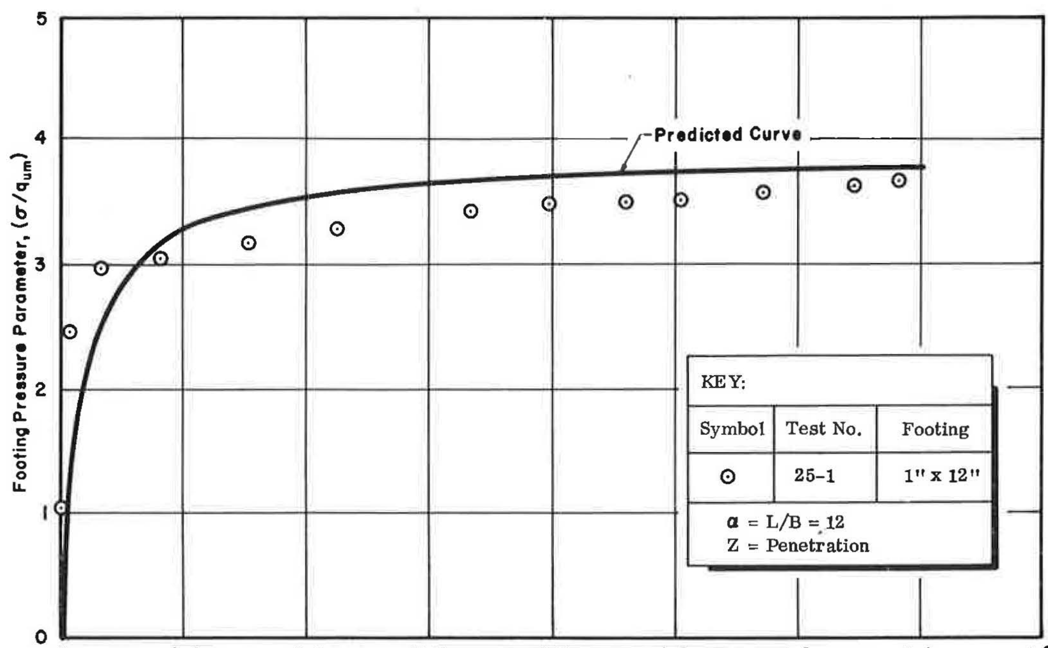

Figure 34. Pressure-penetration relationship for model footings on Grundite (α = 12).

becomes greater. This is in direct contradiction to the data presented herein, as well as both theoretical and experimental bearing capacity results presented by many authors (15, 26, 27).

Reece (22) conducted a similar series of tests on circular and rectangular footings in a cohesive soil. There were several aspects of the study which make comparisons with the results presented herein less useful than one might hope:

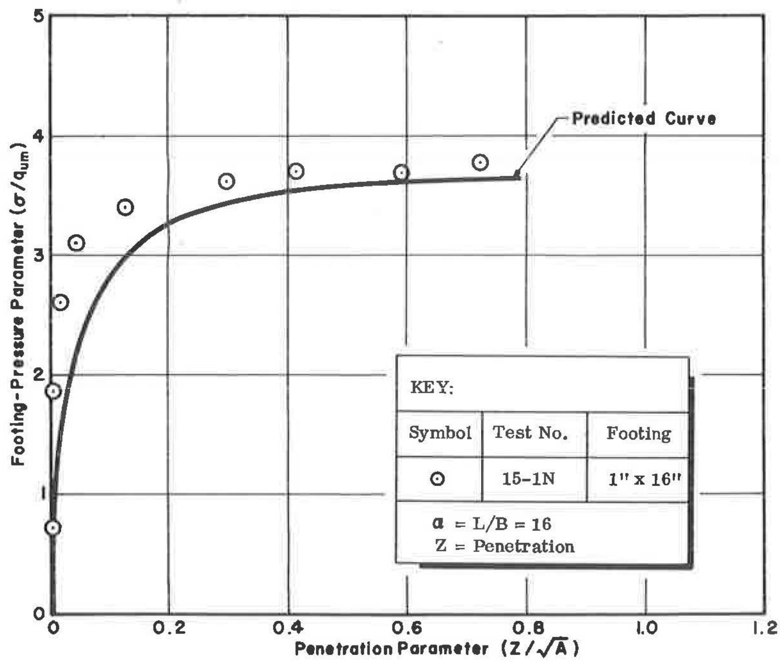

Figure 35. Pressure-penetration relationship for model footings on Grundite (α = 16).

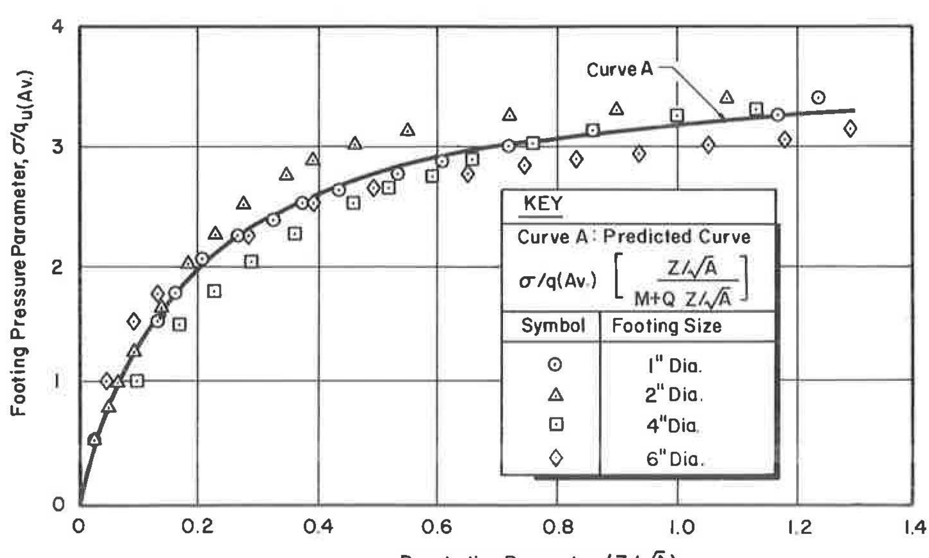

Figure 36. Pressure-penetration relationship for circular footings (data from Reece, 22).

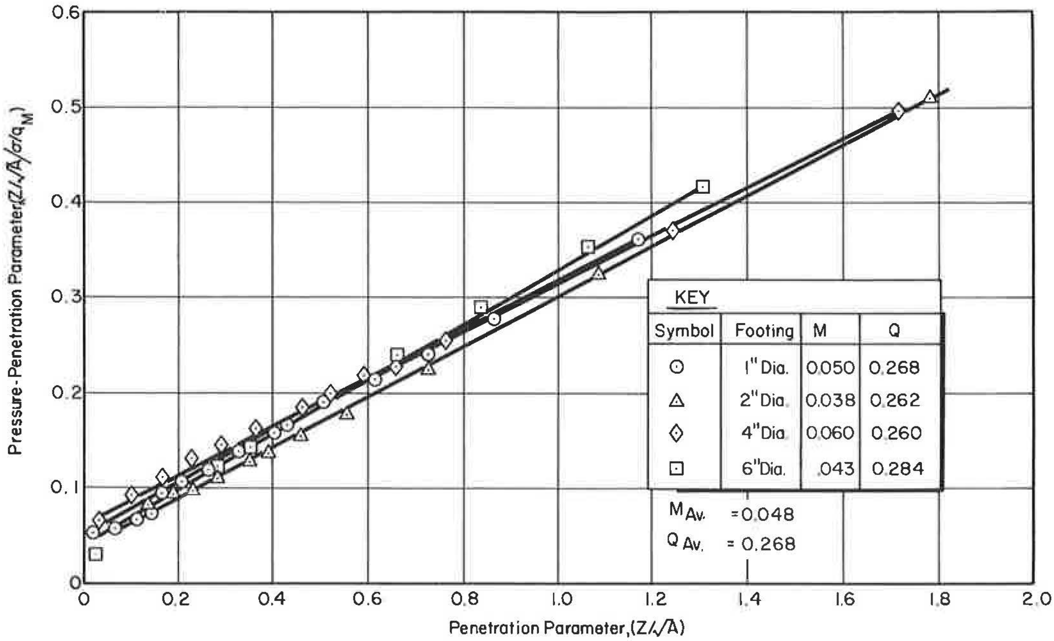

Figure 37. Hyperbolic pressure-penetration test plots for circular footings (data from Reece, 22).

1. The clay soil which Reece (22) used was not completely described, and it is difficult to assess its degree of saturation and other significant properties.

2. The preparation and storage procedures described by Reece (22) hardly seem likely to eliminate experimental scatter due to nonuniformity of the soil. No indication was given of the variability of the strength test results. Furthermore, it appears that the soil strength was not determined in connection with each test series.

3. According to Reece (22), the thickness of the clay layer tested was 13 in. The figures presented by him indicate penetrations of 8 in. and more. It seems almost certain that there was an insufficient depth of clay to prevent an artificial strengthening effect from the underlying sand for the tests on the larger (3- by 18-in., 4- by 18-in.) footings.

Pressure-penetration data for 1-, 2-, 4-, and 6-in. diameter model footings, from Reece (22), are shown in Figure 36. The pressure parameter is given in terms of the average unconfined compressive strength reported by Reece (22), as the individual test results were not presented. The hyperbolic test plot (Fig. 37) indicates the excellent representation of these data by Eq. 6. The solid line in Figure 36 is the plot of Eq. 6 with the constants determined from Figure 37. These results certainly suggest agreement with those presented previously for EPK and Grundite.

It was not possible to evaluate the shape factor variable D, since an adequate number of tests on footings of a given area with varying shape factor were not performed. However, had such data been presented, they would have been suspect because of the difficulty previously cited. To illustrate this point: the results given by Reece (22) for 2- by 9-in., 3- by 13½-in., and 4- by 18-in. footings all substantially coincide with the results in Figure 36. That these curves should, in fact, lie below the data in Figure 36 is predicted by this report, bearing capacity theory (15), and Reece (22, pp. 45-46). This anomaly can readily be explained by the insufficient depth of clay provided.

SUMMARY AND CONCLUSIONS

This paper describes a study of the relationship between the pressure on model footings and their penetration into saturated cohesive soils. Experimental results demonstrate the influence of soil water content, rate of footing penetration, type of testing, and roughness of the footing base on this relationship. An empirical expression has been developed to describe the pressure-penetration relationship. At this time the empirical equation represents the data satisfactorily for square, rectangular, circular, and elliptical model footings of various sizes.

Based on the results of this study, the following conclusions seem justified for the saturated cohesive soils and range of footing sizes and shapes tested:

1. The effect of water content on the pressure-penetration relationship can be greatly reduced, or eliminated, by expressing pressure in terms of a dimensionless pressure parameter, i.e., the footing pressure divided by the mean unconfined compressive strength of the soil, corresponding to the water content of the test.
2. Footing penetration is not, per se, a significant quantity. Rather, it is the penetration in relation to the footing size which is important.
3. The primary influence of the penetration rate on test results appears to stem from moisture migration from the area immediately underneath the footing. For the soils tested, penetration rates equal to or greater than 0. 5 cm/min are sufficiently rapid to prevent significant migration of water from underneath the test footing.
4. The type of testing, i.e., constant rate of penetration or constant rate of loading, has no significant effect providing the average penetration rate is sufficiently rapid to prevent substantial migration of water from underneath the test footing.
5. The roughness of the footing base does not appear to influence the test results. In fact, both smooth and rough base footings seem to develop considerable frictional restraint at the footing-soil interface.
6. An empirical equation has been developed to describe the pressure-penetration relationship for model plate footings on the cohesive soils tested. This equation satisfactorily predicts the behavior of square, rectangular, circular, and elliptical footings of 2 to 27 sq in. in area over a wide range of penetrations. Results of another investigation tend to verify the applicability of the equation, at least for circular footings.
7. The behavior of elliptical footings is identical to that of rectangular footings of the same area with the same length-to-width ratio.

ACKNOWLEDGMENTS

This study was conducted while the senior author was Assistant Professor of Civil Engineering at Ohio State University. The research was supported in part by the Land Locomotion Laboratory of the U. S. Army Tank-Automotive Center under contract DA-33-019-AMC-271T.

REFERENCES

1. Assur, A. Locomotion Over Soft Soil and Snow. SAE Paper 782F, Automotive Eng. Cong., Detroit, Michigan, Jan. 1964.
2. Bekker, M. G. Theory of Land Locomotion, Univ. of Michigan Press. Ann Arbor.
3. Berardi, G. Piastra Rigidia Rettangolare, Caricata Simmetricamente E Appoggiata su un Semipazo Elastico. Giornale del Genio Civile, Vol. 99, No. 11, p. 853, Nov. 1961.
4. Brebner, A., and Wright, W. An Experimental Investigation to Determine the Variation in the Subgrade Modulus of a Sand Loaded by Plates of Different Breadths. Geotechnique, Vol. III, No. 8, Dec. 1953.
5. Carroll, W. F. Vertical Displacements of Spread Footings on Clay: Static and Impulsive Loadings. Unpublished PhD thesis, Univ. of Illinois, Urbana, 1963.
6. Dewhirst, D. L. A Comparison of Pressure Sinkage Size Equations. Chrysler Corp., preprint, May 1964.
7. Janbu, N., Bjerrum, L., and Kjaernsli, B. Veiledning ved løsning av fundamenteringsoppgaver. Norwegian Geotechnical Inst., Publ. No. 16, 1956.
8. Johnson, L. H. Nomography and Empirical Equations, p. 112, John Wiley and Sons, New York, 1952.

9. Karafiath, L. An Analysis of New Techniques for the Estimation of Footing Sinkage in Soils. Land Locomotion Res. Branch, Res. Dev. Div., OTAC, Rept. No. 18, Oct. 1957.
10. Kogler, F. Disc. of Soil Mechanics Research by G. Gilboy. Trans. ASCE, Vol. 98, p. 299, 1933.
11. Kondner, R. L., and Krizek, R. J. Correlation of Load Bearing Tests on Soils. HRB Proc., Vol. 41, p. 557, 1962.
12. Langhaar, H. L. Dimensional Analysis and Theory of Models, John Wiley and Sons, New York, 1951.
13. Matlock, H., Jr., Fenske, C. W., and Dawson, R. F. Deaired Extruded Soil Specimens for Research and for Evaluation of Test Procedures. ASTM Bull. No. 177, Oct. 1951.
14. Mitchell, J. K., and Campanella, R. G. Creep Studies on Saturated Clays. Symp. on Laboratory Shear Testing of Soils, ASTM Spec. Tech. Publ. No. 361, p. 90, 1963.
15. Meyerhof, G. G. The Ultimate Bearing Capacity of Foundations. Geotechnique, Vol. 2, p. 301, 1951.
16. Milne, W. E. Numerical Calculus, Princeton Univ. Press, Princeton, New Jersey, 1949.
17. Osterberg, J. O. Disc. of Symposium on Load Tests of Bearing Capacity of Soils. ASTM Spec. Tech. Publ. No. 79, p. 128, 1948.
18. Osterberg, J. O., and Perloff, W. H. Stress-Strain Characteristics of Compacted Clay Under Varied Rates of Strain. HRB Proc., Vol. 39, p. 605, 1960.
19. Parkes, E. W. A Comparison of the Contact Pressure Beneath Rough and Smooth Rafts on an Elastic Medium. Geotechnique, Vol. 9, p. 183, 1956.
20. Perloff, W. H. A Study of the Pressure-Penetration Relationship for Model Footings on Cohesive Soil. Ohio State Univ. Res. Found. Rept. RF 1745-4, 1964.
21. Rahim, K. S. A. A Theoretical Investigation of Stress Distribution for a Strip Load Placed at Different Depths in an Elastic Half Space. PhD Dissert., Ohio State Univ., 1965.
22. Reece, A. R. Problems of Soil Vehicle Mechanics. Rept. No. 8470, LL 97, U. S. Army Tank-Automotive Center, Warren, Mich., 1964.
23. Schleicher, F. Zur Theorie des Baugrundes. Der Bauingenieur, No. 48, p. 931, 1926.
24. Seed, H. B., Mitchell, J. K., and Chan, C. K. The Strength of Compacted Cohesive Soils. Res. Conf. on Shear Strength of Cohesive Soils, ASCE, p. 877, June 1960.
25. Skempton, A. W. The Bearing Capacity of Clays. British Building Res. Cong., p. 180, 1951.
26. Teng, W. C. Foundation Design, Prentice-Hall, 1962.
27. Terzaghi, K. Theoretical Soil Mechanics, John Wiley and Sons, New York.
28. Trask, P. D., Snow, D. T., et al. Pressure Sinkage Tests on Synthetic and Natural Clay Soils. Land Locomotion Lab., Res. and Eng. Directorate, OTAC, Rept. No. 75, April 1962.
29. Vincent, E. T., Hicks, H. H., Jr., Oktar, E. I., and Kapur, D. K. Rigid Wheel Studies by Means of Dimensional Analysis. Rept. No. 7841, LL 79, U. S. Army Tank-Automotive Center, Center Line, Michigan, 1963.
30. Newmark, N. M. Stress Distribution in Soils. Proc., Purdue Conference on Soil Mechanics and Its Applications, p. 295, 1940.
31. Newmark, N. M. Influence Charts for Computation of Stresses in Elastic Foundations. Bull., Univ. of Illinois Engineering Experiment Sta., No. 338, 1942.